Contribution from the Department of Chemistry
and Molecular Structure Center, Indiana University, Bloomington, Indiana 47405

Tetranuclear Halide–Alkoxide Clusters of Molybdenum Formed by the Coupling of M–M Triple-Bonded Dinuclear Compounds. Synthesis, Characterization, and Molecular Structures of $Mo_4F_2(O\text{-}i\text{-}Pr)_{10}$, $Mo_4X_3(O\text{-}i\text{-}Pr)_9$, and $Mo_4X_4(O\text{-}i\text{-}Pr)_8$ (X = Cl, Br, I)[1]

Malcolm H. Chisholm,* David L. Clark, R. John Errington,[2] Kirsten Folting, and John C. Huffman

Received March 13, 1987

Hydrocarbon solutions of $Mo_2(O\text{-}i\text{-}Pr)_6(M{\equiv}M)$ react with MeCOX or Me_3SiX (GX, 1.5 equiv) to give $Mo_4X_3(O\text{-}i\text{-}Pr)_9$ (I; X = Cl, Br, I) and GO-*i*-Pr. Complexes I may be viewed as the coupled products of $Mo_2X_2(O\text{-}i\text{-}Pr)_4$ and $Mo_2X(O\text{-}i\text{-}Pr)_5$. A further reaction between I and GX (1 equiv) or the direct reaction between $Mo_2(O\text{-}i\text{-}Pr)_6$ and GX (2 equiv) carried out in toluene leads to $Mo_4X_4(O\text{-}i\text{-}Pr)_8$ compounds (II). The compounds II are unstable in solution at elevated temperatures (>60 °C) and react further to give $Mo_4O_2X_2(O\text{-}i\text{-}Pr)_6$ compounds (III) with elimination of *i*-PrX (2 equiv). The ease of the conversion of II to III follows the order X = I > Br > Cl and occurs more readily in CH_2Cl_2 than in hydrocarbon solvents. Attempts to prepare fluoro analogues of II and III by related reaction procedures have failed to give an isolable single product, as did the addition of *i*-PrOH (>8 equiv) to the known compound $Mo_4F_4(O\text{-}t\text{-}Bu)_8$. The reaction between $Mo_2(O\text{-}i\text{-}Pr)_6(M{\equiv}M)$ and 1 equiv of either MeCOF or PF_3 in toluene at −78 °C yielded the thermally unstable, red, crystalline compound $Mo_4F_2(O\text{-}i\text{-}Pr)_{10}$ (IV). Compounds I have been characterized by a variety of spectroscopic techniques and, for X = Br, by a single-crystal X-ray study. Collectively the data present a uniform structural picture involving butterfly Mo_4 units [five Mo–Mo distances of 2.50 Å (averaged) and one long Mo–Mo distance of 3.29 Å] supported by alkoxide bridges, of which two cap the external triangular faces of the butterfly and four edge-bridge backbone and wingtip molybdenum atoms. The wingtip molybdenum atoms have two terminal ligands (X and O-*i*-Pr) while the backbone molybdenum atoms have only one terminal ligand (X or O-*i*-Pr). The local geometry about each molybdenum atom is square pyramidal, MO_4X, where X (Cl or O-*i*-Pr) occupies the apical site. The compounds II show low-temperature limiting ^1H NMR spectra indicative of a butterfly C_{2v} Mo_4 structure related to I by the substitution of the apical O-*i*-Pr ligand on the backbone molybdenum atom by X. The ^1H NMR spectra for II recorded at room temperature indicate O-*i*-Pr ligand scrambling on the NMR time scale. X-ray studies for X = Br confirmed the anticipated butterfly Mo_4 geometry [five Mo–Mo distances of 2.50 Å (averaged) and one Mo-to-Mo distance of 3.2 Å] but, for X = Cl, revealed a square Mo_4 unit (Mo–Mo = 2.38 Å) supported by eight μ-O-*i*-Pr ligands, four above and four below the M_4 plane. The Mo–Cl bonds are terminal and radiate from the center of the square. The square and butterfly Mo_4 units can be viewed as arachno fragments of the well-known *closo*-$Mo_6(\mu_3\text{-}X)_8^{4+}$ moiety. The arachno Mo_4 subunits all have abnormally long radial Mo–L bonds. This phenomenon arises from what is termed the *radial cluster influence*. The compounds III are formulated as derivatives of II in which the two μ_3-O-*i*-Pr ligands are replaced by capping (μ_3) oxo ligands and the backbone molybdenum atoms lack terminal Mo–X bonds. Compound IV contains a rectangular Mo_4 unit having two short, 2.23 Å, and two long, 3.41 Å, distances corresponding to M≡M and nonbonding M-to-M distances, respectively. The M≡M bonds are unbridged, and the tetranuclear compound is viewed as a dimer, $[Mo_2(\mu\text{-}F)(\mu\text{-}O\text{-}i\text{-}Pr)(O\text{-}i\text{-}Pr)_4]_2$. In solution the molecules undergo facile disproportionation to give $Mo_2(O\text{-}i\text{-}Pr)_6$ and other products presumably derived from the reactive species $Mo_2F_2(O\text{-}i\text{-}Pr)_4$. The latter has been trapped, by the addition of PMe_3 (2 equiv) to hydrocarbon solutions of IV, as the adduct $Mo_2F_2(O\text{-}i\text{-}Pr)_4(PMe_3)_2$, for which spectroscopic data indicate a structural analogy to the previously characterized compound $Mo_2F_2(O\text{-}t\text{-}Bu)_4(PMe_3)_2(M{\equiv}M)$. Collectively these studies provide the first examples of the coupling of M–M triple bonds to give 12-electron M_4 clusters. These results are compared to the previously reported condensation of Mo–Mo quadruple bonds. Crystal data: (i) for $Mo_4Br_3(O\text{-}i\text{-}Pr)_9$ at −164 °C, a = 18.645 (7) Å, b = 11.825 (3) Å, c = 19.046 (7) Å, β = 94.64 (2)°, Z = 4, d_{calcd} = 1.833 g cm^{-3}, and space group $P2_1/c$; (ii) for $Mo_4Br_4(O\text{-}i\text{-}Pr)_8$ at −160 °C, a = 20.042 (5) Å, b = 10.980 (2) Å, c = 18.602 (4) Å, β = 112.60 (1)°, Z = 4, d_{calcd} = 2.067 g cm^{-3}, and space group $A2/a$; (iii) for $Mo_4Cl_4(O\text{-}i\text{-}Pr)_8$ at −162 °C, a = 9.971 (10) Å, b = 9.971 (10) Å, c = 18.272 (19) Å, Z = 2, d_{calcd} = 1.825 g cm^{-3}, and space group $I4/m$; (iv) for $Mo_4F_2(O\text{-}i\text{-}Pr)_{10}$ at −160 °C, a = 13.143 (2) Å, b = 10.339 (2) Å, c = 9.088 (1) Å, α = 108.87 (1)°, β = 77.16 (1)°, γ = 113.03 (1)°, Z = 1, and space group $P\bar{1}$.

Introduction

Since our discovery of the M–M triply bonded compounds $M_2(OR)_6$, where M = Mo[3] and W,[4] we have speculated about the coupling of two or more dinuclear units. The M≡M bonds are sterically protected from such oligomerization, and the introduction of small alkoxy substituents undoubtedly leads to the oligomeric compounds $[Mo(OR)_3]_n$, but a detailed knowledge of the structure in the solid state and solution has evaded us.[3,5] It seemed reasonable to suppose that halide-for-alkoxide substitution reactions would also lead to a coupling of the M_2 units since (i) the halides are more electronegative than the alkoxide ligands and (ii) the steric requirements of the halides are less than those of the alkoxide ligand. The challenge then was to design suitable synthetic routes for the stepwise substitution of alkoxides by halides. The obvious route involving the direct addition of anhydrous hydrogen halides is too violent and has several competing side reactions. The best methods seemed to be ones in which an HX-catalyzed sequence could operate (thereby the effective concentration of HX would always be very small) or ones involving bimolecular ligand redistribution reactions.

The reaction between $Mo_2(O\text{-}t\text{-}Bu)_6$ and PF_3 (2 equiv) has been studied previously (eq 1), and the tetranuclear compound $Mo_4(\mu\text{-}F)_4(O\text{-}t\text{-}Bu)_8$ has been fully characterized.[6]

$$2Mo_2(O\text{-}t\text{-}Bu)_6 + 4PF_3 \xrightarrow[\text{hexane}]{22\ ^\circ C} Mo_4F_4(O\text{-}t\text{-}Bu)_8 + 4PF_2(O\text{-}t\text{-}Bu) \quad (1)$$

The central skeleton of this tetranuclear compound is shown in **1**. The molecule may be viewed as two unbridged Mo≡Mo

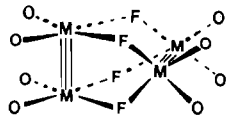

1

bonds, 2.26 Å, brought together via fluoride bridges. The four long Mo-to-Mo distances, ca. 3.75 Å, of the Mo_4 bisphenoid rule

(1) Reactions of Metal–Metal Multiple Bonds. 16. Part 15: Blatchford, T. P.; Chisholm, M. H.; Huffman, J. C. *Inorg. Chem.*, preceding paper in this issue.
(2) Present address: Department of Chemistry, University of Newcastle-upon-Tyne, Newcastle, England.
(3) Chisholm, M. H.; Cotton, F. A.; Murillo, C. A.; Reichert, W. W. *Inorg. Chem.* **1977**, *16*, 1801.
(4) Akiyama, M.; Chisholm, M. H.; Cotton, F. A.; Extine, M. W.; Haitko, D. A.; Little, D. A.; Fanwick, P. E. *Inorg. Chem.* **1979**, *18*, 2266.
(5) Chisholm, M. H.; Huffman, J. C.; Smith, C. A. *J. Am. Chem. Soc.* **1986**, *108*, 222.
(6) Chisholm, M. H.; Clark, D. L.; Huffman, J. C. *Polyhedron* **1985**, *4*, 1203.

0020-1669/88/1327-2071$01.50/0

out any delocalization of M–M bonding. The choice of bridging groups, F rather than *t*-BuO, may be rationalized in terms of the relative π-donating properties of the ligands, *t*-BuO > F, though one could argue that seric factors were also important, at least in terms of assembling a M_4 cluster.

We turned our attention to isopropoxy compounds, for which steric factors would be less important, and we describe here our attempted syntheses of a series of compounds of formula $[Mo(O\text{-}i\text{-}Pr)_2X]_n$, where X = F, Cl, Br, and I, by the coupling of Mo≡Mo units. A preliminary communication has appeared noting the square and butterfly Mo_4 units in the tetranuclear (n = 4) chloro and bromo compounds, respectively.[7]

Syntheses

$Mo_4F_2(O\text{-}i\text{-}Pr)_{10}$. Hydrocarbon solutions of $Mo_2(O\text{-}i\text{-}Pr)_6$ and 1 equiv of either PF_3 or MeCOF react at −78 °C according to eq 2 and 3, respectively.

$$Mo_2(O\text{-}i\text{-}Pr)_6 + PF_3 \xrightarrow[\text{hexane}]{-78\ ^\circ C} {}^1/_2Mo_4F_2(O\text{-}i\text{-}Pr)_{10} + PF_2(O\text{-}i\text{-}Pr) \quad (2)$$

$$Mo_2(O\text{-}i\text{-}Pr)_6 + MeCOF \xrightarrow[\text{hexane}]{-78\ ^\circ C} {}^1/_2Mo_4F_2(O\text{-}i\text{-}Pr)_{10} + MeCO(O\text{-}i\text{-}Pr) \quad (3)$$

If more PF_3 or MeCOF is employed in reactions at −78 °C in hexane, no further F-for-O-*i*-Pr substitution is observed. However, at higher temperatures (>−40 °C) a further reaction does occur but only an intractable green oily material has been obtained in attempted syntheses of $Mo_4F_4(O\text{-}i\text{-}Pr)_8$.

An alternate synthetic approach was tried involving the addition of *i*-PrOH to $Mo_4F_4(O\text{-}t\text{-}Bu)_8$. Alcoholysis readily occurs, but again a green oily compound resulted.

It is possible that in these attempted preparations of $Mo_4F_4(O\text{-}i\text{-}Pr)_8$ a compound of empirical formula $MoF(O\text{-}i\text{-}Pr)_2$ is formed, but it is also clear that this must be quite different from the other halides of related empirical formula. The complexity of the NMR spectra (^1H and ^{19}F) suggest that more than one compound (isomer) must be present and further that MeCO(O-*i*-Pr) or $PF_2(O\text{-}i\text{-}Pr)$ can coordinate.

The compound $Mo_4F_2(O\text{-}i\text{-}Pr)_{10}$ is thermally unstable above −20 °C in hydrocarbon solvents but stable in the crystalline state at ambient temperature. In solution it undergoes a ligand redistribution reaction, yielding $Mo_2(O\text{-}i\text{-}Pr)_6$ and a green oily substance similar to that noted above. Addition of PMe_3 (2 equiv) to a hexane solution at −78 °C leads to cleavage as shown in eq 4. The resultant compound $Mo_2F_2(O\text{-}i\text{-}Pr)_4(PMe_3)_2$ is spectroscopically analogous to the previously characterized compound $Mo_2F_2(O\text{-}t\text{-}Bu)_4(PMe_3)_2$.[6]

$$Mo_4F_2(O\text{-}i\text{-}Pr)_{10} + 2PMe_3 \xrightarrow[\text{hexane}]{-78\ ^\circ C} Mo_2F_2(O\text{-}i\text{-}Pr)_4(PMe_3)_2 + Mo_2(O\text{-}i\text{-}Pr)_6 \quad (4)$$

The compound $Mo_4F_2(O\text{-}i\text{-}Pr)_{10}$ was obtained in ca. 70% crystalline yield according to the stoichiometry shown in eq 2 and 3. The dark red crystals are air-sensitive and must be handled under a dry and oxygen-free atmosphere (N_2). Because the compound is thermally unstable in solution, a low-temperature reaction vessel was designed for its synthesis.

$Mo_4X_3(O\text{-}i\text{-}Pr)_9$ (I). Reactions between $Mo_2(O\text{-}i\text{-}Pr)_6$ and either acetyl halides or trimethylsilyl halides lead to halide-for-alkoxide exchange as noted in eq 5.

$$2Mo_2(O\text{-}i\text{-}Pr)_6 + 3GX \xrightarrow[\text{hexane}]{t\ ^\circ C} Mo_4X_3(O\text{-}i\text{-}Pr)_9 + 3GO\text{-}i\text{-}Pr \quad (5)$$

G = Me_3Si, MeCO

For each reagent the reactivities increase with decreasing strength of the element (C or Si)-to-halogen bond; i.e., the rates follow the order I > Br > Cl, and the rates of reaction are more rapid for G = MeCO than for Me_3Si. Thus, while acetyl chloride reacts quite rapidly at room temperature, Me_3SiCl does not show any significant reaction below +40 °C. The reactions involving both MeCOBr and Me_3SiBr proceed quite rapidly at room temperature with notable evolution of heat, while the iodo derivatives are best prepared by initiating the reactions at −78 °C and allowing the solutions to warm to room temperature slowly.

The compounds I are only sparingly soluble in hexane and may readily be crystallized from this solvent. The compounds I are appreciably more soluble in toluene and react further with GX according to eq 6.

$$Mo_4X_3(O\text{-}i\text{-}Pr)_9 + GX \xrightarrow[\text{toluene}]{22\ ^\circ C} Mo_4X_4(O\text{-}i\text{-}Pr)_8 + GO\text{-}i\text{-}Pr \quad (6)$$

The compounds $Mo_4X_4(O\text{-}i\text{-}Pr)_8$ (II) can be prepared directly in toluene by the stoichiometric reaction shown in eq 7. Again

$$2Mo_2(O\text{-}i\text{-}Pr)_6 + 4GX \xrightarrow[\text{toluene}]{t\ ^\circ C} Mo_4X_4(O\text{-}i\text{-}Pr)_8 + 4GO\text{-}i\text{-}Pr \quad (7)$$

G = Me_3Si, MeCO

the reaction temperatures for eq 7 follows the factors noted for eq 5. NMR studies of the reactions between $Mo_2(O\text{-}i\text{-}Pr)_6$ and GX in toluene-d_8 indicate that I is formed even at very low concentrations of GX and that II is formed from I as shown in eq 6.

The successful isolation of I rests on crystallization from hexane. The compounds II are thermally unstable in solution and react to give III according to the stoichiometric reaction shown in eq 8.

$$Mo_4X_4(O\text{-}i\text{-}Pr)_8 \xrightarrow[\text{toluene}]{t\ ^\circ C} Mo_4O_2X_2(O\text{-}i\text{-}Pr)_6 + 2i\text{-}PrX \quad (8)$$

The thermal stability of II is in the order X = Cl > Br > I with the chloro and bromo compounds being stable for several days in toluene at room temperature but reacting at a significant rate at temperatures in the range 50–80 °C. The iodo compound slowly decomposes even at room temperature to give $Mo_4O_2I_2(O\text{-}i\text{-}Pr)_6$. In the polar solvent CH_2Cl_2 the conversion of II to III becomes more rapid. In general the solubilities follow the order X = I > Br > Cl and aromatic > aliphatic hydrocarbons.

Mechanistic Considerations concerning Halide-for-Alkoxide Exchange at the Mo_2^{6+} Center. During the course of this study it was discovered that trace amounts of alcohol accelerated the reaction between $Mo_2(O\text{-}i\text{-}Pr)_6$ and either MeCOX or Me_3SiX. This observation forms the basis for the proposal of a generalized alcohol-catalyzed reaction sequence followed by the coupling of two Mo_2 units outlined by eq 9–11. The equilibria shown in eq

$$GX + i\text{-}PrOH \rightleftharpoons GO\text{-}i\text{-}Pr + HX \quad (9)$$

$$Mo_2(O\text{-}i\text{-}Pr)_6 + HX \rightarrow Mo_2X(O\text{-}i\text{-}Pr)_5 + HO\text{-}i\text{-}Pr \quad (10a)$$

$$Mo_2X(O\text{-}i\text{-}Pr)_5 + HX \rightarrow Mo_2X_2(O\text{-}i\text{-}Pr)_4 + HO\text{-}i\text{-}Pr \quad (10b)$$

$$Mo_4X_3(O\text{-}i\text{-}Pr)_9 + HX \rightarrow Mo_4X_4(O\text{-}i\text{-}Pr)_8 + HO\text{-}i\text{-}Pr \quad (10c)$$

$$2Mo_2X(O\text{-}i\text{-}Pr)_5 \rightarrow Mo_4X_2(O\text{-}i\text{-}Pr)_{10} \quad (11a)$$

$$Mo_2X(O\text{-}i\text{-}Pr)_5 + Mo_2X_2(O\text{-}i\text{-}Pr)_4 \rightarrow Mo_4X_3(O\text{-}i\text{-}Pr)_9 \quad (11b)$$

9 are well established for G = MeCO and Me_3Si and could also be operative for G = PF_2.[8-11] The second step in the reaction sequence, eq 10, leads to the halide-for-alkoxide exchange at the

(7) Chisholm, M. H.; Errington, R. J.; Folting, K.; Huffman, J. C. *J. Am. Chem. Soc.* **1982**, *104*, 2025.

(8) Jung, M. E.; Ornstein, P. L. *Tetrahedron Lett.* **1972**, *31*, 2659. Jung, M. E.; Hatfield, G. L. *Tetrahedron Lett.* **1978**, *46*, 4483.

(9) Patai, S. In *The Chemistry of the Hydroxyl Group*; Interscience: New York, 1971; Chapter 11, p 593.

(10) Satchell, D. P. N.; Satchell, R. S. In *The Chemistry of Acyl Halides*; Patai, S., Ed.; Interscience: New York, 1972; Chapter 4, p 103.

(11) Emsley, J.; Hall, D. In *The Chemistry of Phosphorus*; Harper and Row: London, 1976.

Scheme I

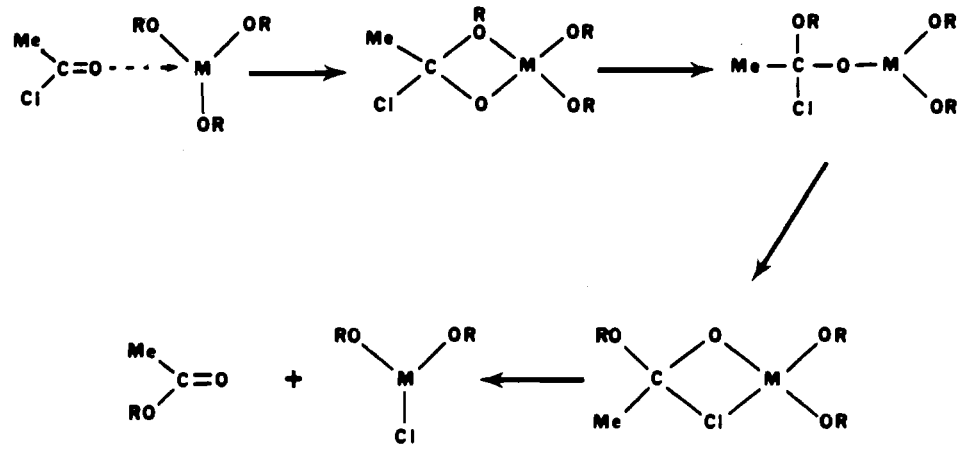

molybdenum centers and regenerates the alcohol. The associative steps, eq 11, lead to the tetranuclear complexes and presumably are controlled by steric factors and the Lewis acidity of the metal centers.

It should be noted that trace quantities of ROH and Me_2NH always exist in hydrocarbon solutions of metal alkoxides and metal amides, respectively, due to adventitious hydrolysis and they have been previously determined to be responsible for catalyzed CO_2 insertion reactions[12] and Cl-for-NMe_2 exchange reactions.[13] It is, of course, possible that a direct substitution pathway is also operative but kinetically slower. When reactions between $Mo_2(O\text{-}i\text{-}Pr)_6$ and MeCOCl were followed in NMR-tube reactions with toluene-d_8 as solvent in the presence of Proton Sponge (1,8-bis(dimethylamino)naphthalene), the $t_{1/2}$ values for the reaction were ca. 3 times greater than those carried out in the absence of the HCl scavenger. The failure of Proton Sponge to suppress the reaction completely could be interpreted in terms of either the existence of a direct substitution mechanism or its failure to scavenge all the available HX molecules. A plausible direct mechanism is shown in the reaction sequence in Scheme I.

Pertinent to the proposal that discrete $Mo_2Cl(O\text{-}i\text{-}Pr)_5$ and $Mo_2Cl_2(O\text{-}i\text{-}Pr)_4$ units are formed and then couple (eq 11b) is the finding that $Mo_2(O\text{-}i\text{-}Pr)_6$ and PMe_2Cl (2 equiv) react according to eq 12. The NMR characterization data for $Mo_2Cl_2(O\text{-}i\text{-}Pr)_4(PMe_2(O\text{-}i\text{-}Pr))_2$ leave no doubt that this is analogous to the structurally characterized compounds $M_2F_2(O\text{-}t\text{-}Bu)_4(PMe_3)_2$ having unbridged M≡M bonds uniting four-coordinate metal centers.

$$Mo_2(O\text{-}i\text{-}Pr)_6 + 2PMe_2Cl \xrightarrow[\text{toluene}]{22\ ^\circ C} Mo_2Cl_2(O\text{-}i\text{-}Pr)_4(PMe_2(O\text{-}i\text{-}Pr))_2 \quad (12)$$

Solid-State and Molecular Structures

Four tetranuclear compounds have been examined by single-crystal X-ray studies during this work: $Mo_4F_2(O\text{-}i\text{-}Pr)_{10}$, $Mo_4Br_3(O\text{-}i\text{-}Pr)_9$, $Mo_4Cl_4(O\text{-}i\text{-}Pr)_8$, and $Mo_4Br_4(O\text{-}i\text{-}Pr)_8$. In each case the unit cell revealed discrete molecules. A summary of data collection and crystallographic parameters is given in Table I. Atomic positional parameters are given in Tables II–V.

$Mo_4F_2(O\text{-}i\text{-}Pr)_{10}$. A ball and stick drawing giving the atom-numbering scheme for this centrosymmetric molecule is given in Figure 1.

The molecule may be viewed as a dimer, $[Mo_2(\mu\text{-}F)(\mu\text{-}O\text{-}i\text{-}Pr)(O\text{-}i\text{-}Pr)_4]_2$, and the centrosymmetric structure is presumably favored over a molecule having C_{2v} symmetry on steric grounds. There is a rectangle of molybdenum atoms with two short Mo–Mo distances, 2.23 Å, corresponding to localized Mo–Mo triple bonds, and two long, nonbonding Mo–Mo distances, 3.41 Å. The rectangular Mo_4 unit provides an alternative to the bisphenoid Mo_4 unit in $Mo_4F_4(O\text{-}t\text{-}Bu)_8$ in preserving the two discrete Mo≡Mo bonds. The local geometry for the $Mo_4F_2O_{10}$ moiety is similar to that found by McCarley[14] for the $[P_2Cl_2Mo_2(\mu\text{-}Cl_2)]_2$ unit in $Mo_4Cl_8(PPh_3)_4$, which is formed by the condensation of two Mo–Mo quadruple bonds (eq 13), though in the latter there is cluster bonding in the rectangular unit as a result of the overlap of the four Mo δ orbitals.

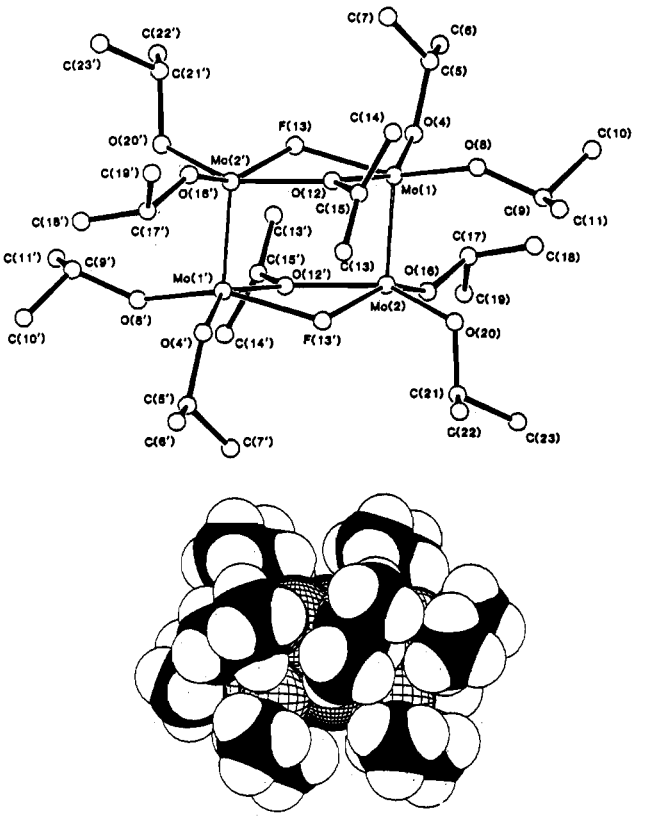

Figure 1. Ball-and-stick view of the $Mo_4(\mu\text{-}F)_2(\mu\text{-}O\text{-}i\text{-}Pr)_2(O\text{-}i\text{-}Pr)_8$ molecule emphasizing the near-square-planar geometry about each Mo atom and giving the numbering scheme used in the tables. A space-filling model diagram of the same view is shown at the bottom of the figure.

$$2Mo_2Cl_4(PPh_3)_2(MeOH)_2 \rightarrow Mo_4Cl_8(PPh_3)_4 + 4MeOH \quad (13)$$

Selected bond distances and bond angles for $Mo_4F_2(O\text{-}i\text{-}Pr)_{10}$ are given in Tables VI and VII, respectively. The terminal Mo–O bond distances fall into two types averaging 1.88 and 1.91 Å for the Mo–O bonds trans to the bridging Mo–F and Mo–O bonds, respectively. Both distances are short and are in the range found

(12) Chisholm, M. H.; Extine, M. W. *J. Am. Chem. Soc.* **1977**, *99*, 792.
(13) Akiyama, M.; Chisholm, M. H.; Cotton, F. A.; Extine, M. W.; Murillo, C. A. *Inorg. Chem.* **1977**, *16*, 2407.
(14) McGinnis, R. N.; Ryan, T. R.; McCarley, R. E. *J. Am. Chem. Soc.* **1978**, *100*, 7900.

Table I. Summary of Crystallographic Data[a]

	I	II	III	IV
empirical formula	$Mo_4C_{30}H_{70}F_2O_{10}$	$Mo_4Br_3(OCH(CH_3)_2)_9$	$Mo_4Cl_4O_8C_{24}H_{56}$	$Mo_4Br_4O_8C_{24}H_{56}$
color of cryst	black		black	black (green)
cryst dimens, mm	0.23 × 0.25 × 0.25	0.20 × 0.28 × 0.32	0.14 × 0.14 × 0.14	0.12 × 0.12 × 0.13
space group	$P\bar{1}$	$P2_1/c$	$I4/m$	$A2/a$
cell dimens				
temp, °C	−160	−164	−162	−160
a, Å	13.143 (2)	18.645 (7)	9.971 (10)	20.042 (5)
b, Å	10.339 (2)	11.825 (3)	9.971 (10)	10.980 (2)
c, Å	9.088 (1)	19.046 (7)	18.272 (19)	18.602 (4)
α, deg	108.87 (1)			
β, deg	77.16 (1)	94.64 (2)		112.60 (1)
γ, deg	113.03 (1)			
Z, molecules/cell	1	4	2	4
vol, Å^3	1068.97	4185.35	1816.43	3779.26
calcd density, g/cm^3	1.573	1.833	1.825	2.067
wavelength, Å	0.71069	0.71069	0.71069	0.71069
mol wt	1012.63	1155.26	998.27	1176.08
linear abs coeff, cm^{-1}	11.712	40.216	16.546	54.954
detector to sample dist, cm	22.5	22.5	22.5	22.5
sample to source dist, cm	23.5	23.5	23.5	23.5
av ω-scan width at half-height	0.25	0.25	0.25	0.25
scan speed, deg/min	4.0	5.0	3.0	3.0
scan width (+dispersion), deg	2.0	1.8	2.0	2.0
individual bkgd, s	6	4	5	5
aperture size, mm	3.0 × 4.0	4.0 × 4.0	3.0 × 4.0	3.0 × 4.0
2θ range, deg	6–45	6–45	5–50	6–50
total no. of reflns collected	3683	6803	1959	4147
no. of unique intens	2803	5493	846	3338
no. with $F > 0.0$		5132	761	3146
no. with $F > \sigma(F)$		4898	693	
no. with $F > 2.33\sigma(F)$		4525	592	2863
no. with $F > 3.00\sigma(F)$	2661			
$R(F)$	0.0337	0.0577	0.045	0.0376
$R_w(F)$	0.0450	0.0558	0.040	0.0363
goodness of fit for the last cycle	1.526	1.236	0.859	1.183
max Δ/σ for last cycle	0.05	0.05	0.05	0.05

[a] Abbreviations: I = $Mo_4F_2(O\text{-}i\text{-}Pr)_{10}$; II = $Mo_4Br_3(O\text{-}i\text{-}Pr)_9$; III = $Mo_4Cl_4(O\text{-}i\text{-}Pr)_8$; IV = $Mo_4Br_4(O\text{-}i\text{-}Pr)_8$.

Table II. Fractional Coordinates and Isotropic Thermal Parameters for the $Mo_4F_2(O\text{-}i\text{-}Pr)_{10}$ Molecule

atom	10^4x	10^4y	10^4z	$10B_{iso}$, Å^2
Mo(1)	6388.1 (3)	295.0 (5)	−1558.0 (5)	16
Mo(2)	6431.0 (3)	561.2 (4)	969.2 (5)	13
F(3)	5089 (2)	1076 (3)	−1323 (3)	17
O(4)	7288 (3)	2250 (4)	−1619 (4)	22
C(5)	7286 (5)	2686 (7)	−2964 (7)	32
C(6)	7064 (6)	4112 (7)	−2395 (8)	46
C(7)	8371 (6)	2789 (10)	−3970 (8)	56
O(8)	7333 (3)	−736 (4)	−2727 (4)	23
C(9)	8171 (5)	−1279 (7)	−2633 (6)	32
C(10)	8314 (6)	−2389 (7)	−4160 (1)	51
C(11)	9163 (6)	−138 (9)	−2164 (12)	65
O(12)	4857 (3)	−1438 (3)	−1934 (4)	18
C(13)	4654 (8)	−2985 (8)	−2477 (14)	87
C(14)	4178 (6)	−3628 (8)	−3976 (9)	58
C(15)	5027 (12)	−3637 (8)	−1746 (9)	92
O(16)	7649 (3)	2246 (4)	1616 (4)	18
C(17)	8687 (4)	3201 (5)	1061 (6)	18
C(18)	8706 (5)	4748 (6)	1708 (8)	35
C(19)	9611 (5)	2991 (7)	1589 (8)	34
O(20)	7044 (3)	−899 (4)	758 (4)	22
C(21)	7329 (6)	−1063 (8)	2133 (8)	44
C(22)	6531 (7)	−1036 (1)	3450 (8)	59
C(23)	7741 (6)	−2318 (8)	1574 (8)	41

for significant O-to-Mo π-bonding.[15] The Mo–O–C angles associated with the shorter Mo–O bonds are larger, ca. 144°, than those associated with the longer distances, ca. 120°, as is generally found in compounds where O-to-Mo π-bonding is important.[15] There is little asymmetry in the $Mo_2(\mu\text{-}F)$ and $Mo_2(\mu\text{-}O\text{-}i\text{-}Pr)$ moieties, and the distances and angles are similar to those found in $Mo_4F_4(O\text{-}t\text{-}Bu)_8$.[6]

(15) Chisholm, M. H. *Polyhedron* **1983**, *2*, 681.

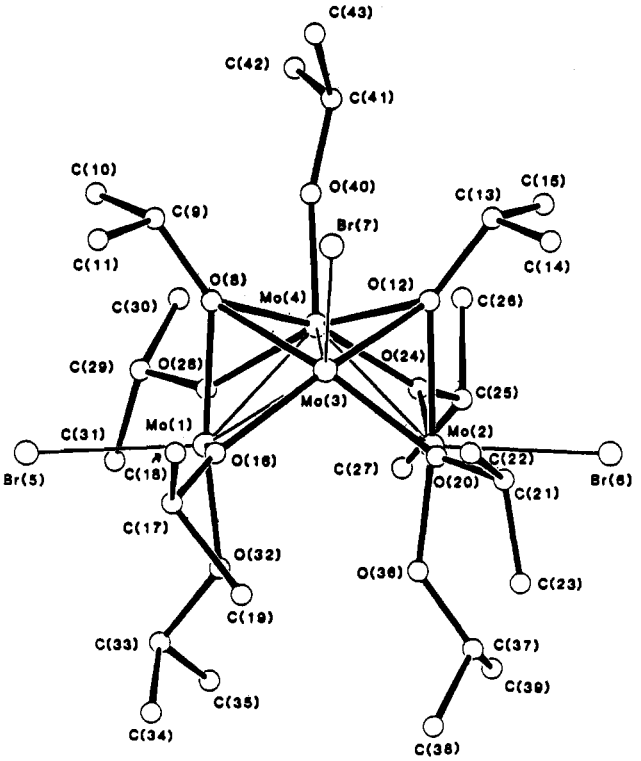

Figure 2. View of the $Mo_4Br_3(O\text{-}i\text{-}Pr)_9$ molecule parallel to the mirror plane bisecting the backbone of the Mo_4 butterfly unit, giving the atom-numbering scheme used in the tables.

$Mo_4Br_3(O\text{-}i\text{-}Pr)_9$. Selected bond distances and bond angles are given in Tables VIII and IX, respectively, and a view of the

Table III. Fractional Coordinates and Isotropic Thermal Parameters for the $Mo_4Br_3(O\text{-}i\text{-}Pr)_9$ Molecule

atom	10^4x	10^4y	10^4z	$10B_{iso}$, Å^2
Mo(1)	2104.6 (5)	210 (1)	9203.0 (5)	13
Mo(2)	2496 (1)	326 (1)	7553.7 (5)	15
Mo(3)	3167.6 (5)	−510 (1)	8619.8 (5)	13
Mo(4)	2904 (1)	1563 (1)	8598 (1)	11
Mo(4)*	1925 (4)	−1153 (6)	8260 (3)	18
Br(5)	1711 (1)	111 (1)	10489 (1)	23
Br(6)	2732 (1)	490 (1)	6230 (1)	27
Br(7)	4437 (1)	−1320 (1)	8987 (1)	24
Br(1)*	1379 (5)	−3131 (8)	7993 (5)	31
O(8)	3207 (4)	541 (6)	9504 (4)	17
C(9)	3721 (6)	739 (10)	10148 (5)	17
C(10)	3482 (7)	1800 (12)	10517 (7)	35
C(11)	3734 (6)	−282 (12)	10607 (6)	26
O(12)	3597 (4)	678 (6)	7933 (4)	17
C(13)	4305 (7)	932 (12)	7683 (7)	31
C(14)	4551 (8)	−72 (15)	7274 (8)	45
C(15)	4244 (8)	1947 (14)	7328 (8)	47
O(16)	2521 (4)	−1387 (6)	9259 (4)	17
C(17)	2336 (10)	−2403 (12)	9578 (9)	51
C(18)	2964 (9)	−3137 (14)	9760 (9)	55
C(19)	1893 (11)	−3068 (17)	8898 (12)	73
O(20)	2900 (4)	−1281 (6)	7660 (4)	18
C(21)	3085 (7)	−2189 (12)	7189 (7)	31
C(22)	3501 (9)	−3041 (13)	7565 (9)	51
C(23)	2399 (10)	−2619 (15)	6831 (8)	54
O(24)	2423 (4)	2025 (7)	7637 (4)	27
C(25)	2168 (7)	2972 (11)	7226 (5)	25
C(26)	2667 (7)	3940 (11)	7353 (7)	30
C(27)	1398 (8)	3225 (13)	7398 (7)	39
O(28)	2061 (4)	1907 (7)	9180 (4)	20
C(29	1815 (6)	2793 (10)	9619 (6)	20
C(30)	2146 (7)	3911 (10)	9422 (6)	24
C(31)	1011 (7)	2845 (11)	9543 (6)	28
O(32)	1188 (4)	−115 (7)	8790 (4)	24
C(33)	456 (6)	−1230 (11)	9005 (6)	26
C(34)	194 (6)	−1288 (11)	9031 (7)	29
C(35)	9 (7)	620 (12)	8481 (7)	35
O(36)	1532 (4)	−56 (7)	7363 (4)	27
C(37)	1073 (7)	−371 (12)	6743 (6)	35
C(38)	647 (8)	650 (14)	6487 (8)	47
C(39)	619 (9)	−1319 (15)	6927 (9)	53
O(40)	3657 (4)	2631 (8)	8892 (5)	19
C(41)	4257 (8)	3322 (15)	8923 (10)	49
C(42)	4096 (9)	4487 (13)	9147 (9)	34
C(43)	4916 (9)	2811 (14)	9255 (9)	41

Table IV. Fractional Coordinates and Isotropic Thermal Parameters for the $Mo_4Cl_4(O\text{-}i\text{-}Pr)_8$ Molecule[a]

atom	10^4x	10^4y	10^4z	$10B_{iso}$, Å^2
Mo(1)	5000*	5000*	5909 (1)	39
Mo(2)	3294 (1)	4938 (2)	5000*	20
Cl(3)	5000*	5000*	7245 (2)	49
Cl(4)	857 (4)	5046 (5)	5000*	31
O(5)	6311 (4)	6488 (4)	5847 (2)	27
C(6)	7065 (8)	7330 (8)	6368 (5)	44
C(7)	8260 (9)	7899 (11)	6000 (6)	57
C(8)	6152 (14)	8382 (16)	6659 (9)	77

[a] Asterisks denote coordinates that are crystallographically defined.

molecule giving the atom-numbering scheme and looking parallel to the mirror plane containing the backbone of the Mo_4 butterfly is shown in Figure 2.

In the solid state, the $Mo_4Br_3(O\text{-}i\text{-}Pr)_9$ molecule has virtual C_s symmetry. The four molybdenum atoms form a butterfly or opened tetrahedron with five relatively short Mo–Mo distances, 2.51 Å (average), and one long Mo-to-Mo distance, 3.29 Å. The local $MoBrO_4$ geometry (or MoO_5 for the unique Mo atom) corresponds to a square-based pyramid with apical, terminal Mo–Br bonds of 2.60 Å (average). There are three types of bonding modes for the O-*i*-Pr ligands. A pair of symmetry-related μ_3-O-*i*-Pr ligands cap the triangular faces of the Mo_4 butterfly, Mo–O = 2.14 Å (average). There are two symmetry-related pairs of μ-O-*i*-Pr ligands that bridge four edges of the Mo_4 moiety,

Table V. Fractional Coordinates and Isotropic Thermal Parameters for the $Mo_4Br_4(O\text{-}i\text{-}Pr)_8$ Molecule

atom	10^4x	10^4y	10^4z	$10B_{iso}$, Å^2
Mo(1)	3380.8 (3)	1439.3 (5)	477.9 (3)	7
Mo(2)	2587.0 (3)	2753.4 (5)	−625.3 (3)	7
Br(3)	4774.5 (3)	1288 (1)	1189.6 (4)	13
Br(4)	2690.7 (3)	4801 (1)	−1241.4 (4)	13
O(5)	3254 (2)	−225 (4)	423 (2)	10
C(6)	3690 (4)	−1289 (6)	768 (4)	16
C(7)	3902 (4)	−1908 (7)	164 (5)	22
C(8)	3250 (5)	−2110 (7)	1078 (5)	21
O(9)	3355 (2)	3404 (4)	470 (2)	9
C(10)	3833 (3)	4465 (6)	749 (4)	12
C(11)	4196 (4)	4430 (8)	1619 (4)	17
C(12)	4374 (4)	4477 (7)	369 (4)	15
C(13)	3213 (2)	1791 (4)	1461 (2)	10
C(14)	3635 (3)	1728 (6)	2297 (4)	13
C(15)	3778 (4)	402 (7)	2523 (4e	16
C(16)	3232 (4)	2357 (7e	2737 (4)	18
O(17)	3484 (22)	1808 (4)	−539 (2)	9
C(18)	3907 (4)	1350 (6)	−965 (4)	13
C(19)	4071 (4)	2384 (7)	−1412 (5)	21
C(20)	3496 (4)	328 (6)	−1487 (4)	16

Table VI. Selected Bond Distances (Å) for the $Mo_4(\mu\text{-}F)_2(\mu\text{-}O\text{-}i\text{-}Pr)_2(O\text{-}i\text{-}Pr)_8$ Molecule

Mo(1)–Mo(2)	2.2339 (7)	Mo(2)–F(13)	2.0930 (26)
Mo(1)–F(13)	2.1023 (26)	Mo(2)–O(12)	2.117 (3)
Mo(1)–O(4)	1.913 (3)	Mo(2)–O(16)	1.875 (3)
Mo(1)–O(8)	1.877 (3)	Mo(2)–O(20)	1.913 (3)
Mo(1)–O(12)	2.113 (3)		

Table VII. Selected Bond Angles (deg) for the $Mo_4(\mu\text{-}F)_2(\mu\text{-}O\text{-}i\text{-}Pr)_2(O\text{-}i\text{-}Pr)_8$ Molecule

Mo(2)–Mo(1)–F(3)	98.64 (7)	Mo(1)–Mo(2)–O(12)	98.84 (9)
Mo(2)–Mo(1)–O(4)	97.65 (10)	Mo(1)–Mo(2)–O(16)	106.45 (10)
Mo(2)–Mo(1)–O(8)	107.59 (11)	Mo(1)–Mo(2)–O(20)	99.19 (11)
Mo(2)–Mo(1)–O(12)	99.84 (10)	F(3)–Mo(2)–O(12)	68.94 (12)
F(3)–Mo(1)–O(4)	82.44 (3)	F(3)–Mo(2)–O(16)	154.49 (13)
F(3)–Mo(1)–O(8)	152.47 (13)	F(3)–Mo(2)–O(20)	83.77 (13)
F(3)–Mo(1)–O(12)	68.86 (11)	O(12)–Mo(2)–O(16)	98.77 (13)
O(4)–Mo(1)–O(8)	101.81 (16)	O(12)–Mo(2)–O(20)	148.98 (14)
O(4)–Mo(1)–O(12)	148.21 (14)	O(16)–Mo(2)–O(20)	100.04 (15)
O(8)–Mo(1)–O(12)	97.92 (14)	Mo(1)–F(3)–Mo(2)	108.94 (11)
Mo(1)–Mo(2)–F(3)	97.70 (8)	Mo(1)–O(12)–Mo(2)	107.63 (14)

Table VIII. Selected Bond Distances (Å) for the $Mo_4Br_3(O\text{-}i\text{-}Pr)_9$ Molecule

Mo(1)–Mo(3)	2.499 (2)	Mo(2)–O(36)	1.860 (7)
Mo(1)–Mo(4)	2.527 (2)	Mo(3)–Mo(4)	2.500 (2)
Mo(1)–Br(5)	2.615 (2)	Mo(3)–Br(7)	2.596 (2)
Mo(1)–O(8)	2.126 (7)	Mo(3)–O(8)	2.090 (7)
Mo(1)–O(16)	2.041 (7)	Mo(3)–O(12)	2.121 (7)
Mo(1)–O(28)	2.008 (8)	Mo(3)–O(16)	2.061 (7)
Mo(1)–O(32)	1.862 (7)	Mo(3)–O(20)	2.067 (7)
Mo(2)–Mo(3)	2.502 (2)	Mo(4)–O(8)	2.144 (7)
Mo(2)–Mo(4)	2.536 (2)	Mo(4)–O(12)	2.154 (7)
Mo(2)–Br(6)	2.602 (2)	Mo(4)–O(24)	2.047 (7)
Mo(2)–O(12)	2.162 (7)	Mo(4)–O(28)	2.035 (7)
Mo(2)–O(20)	2.048 (7)	Mo(4)–O(40)	1.938 (9)
Mo(2)–O(24)	2.020 (9)		

Mo–O = 2.04 Å (average). Note the backbone is not bridged. There are three terminal Mo–O-*i*-Pr ligands, two being bonded to the wingtip Mo atoms, Mo–O = 1.86 Å and Mo–O–C = 136.5° (averaged), and the other to a backbone Mo atom, Mo–O = 1.94 Å and Mo–O–C = 164.2°. The correlation of Mo–O distance and Mo–O–C angle is not what is normally seen.[15] Steric factors appear important in a repulsive interaction across the wingtip Mo atoms, and this is seen in space-filling drawings of the molecule. The rather long Mo–O terminal distance, 1.94 Å, and the long Mo–Br distances are attributed to a *radial cluster influence*, and this is discussed in the following paper, which deals with the electronic structure and bonding in these 12-electron Mo_4 clusters.

$Mo_4Br_4(O\text{-}i\text{-}Pr)_8$. Selected bond distances and bond angles are given in Tables X and XI, respectively, and an ORTEP view

Table IX. Selected Bond Angles (deg) for the $Mo_4Br_3(O\text{-}i\text{-}Pr)_9$ Molecule

Mo(3)–Mo(1)–Mo(4)	59.7 (0)	Mo(2)–Mo(3)–O(20)	53.2 (2)
Mo(3)–Mo(1)–Br(5)	133.9 (1)	Mo(4)–Mo(3)–Br(7)	122.7 (1)
Mo(3)–Mo(1)–O(8)	53.0 (2)	Mo(4)–Mo(3)–O(8)	54.8 (2)
Mo(3)–Mo(1)–O(16)	52.8 (2)	Mo(4)–Mo(3)–O(12)	54.8 (2)
Mo(3)–Mo(1)–O(28)	111.3 (2)	Mo(4)–Mo(3)–O(16)	112.3 (2)
Mo(3)–Mo(1)–O(32)	118.4 (2)	Mo(4)–Mo(3)–O(20)	112.6 (2)
Mo(4)–Mo(1)–Br(5)	132.5 (1)	Br(7)–Mo(3)–O(8)	91.8 (2)
Mo(4)–Mo(1)–O(8)	54.1 (2)	Br(7)–Mo(3)–O(12)	91.7 (2)
Mo(4)–Mo(1)–O(16)	111.9 (2)	Br(7)–Mo(3)–O(16)	102.7 (2)
Mo(4)–Mo(1)–O(28)	51.8 (2)	Br(7)–Mo(3)–O(20)	103.0 (2)
Mo(4)–Mo(1)–O(32)	119.5 (3)	O(8)–Mo(3)–O(21)	96.5 (3)
Br(5)–Mo(1)–O(8)	95.4 (2)	O(8)–Mo(3)–O(16)	78.9 (3)
Br(5)–Mo(1)–O(16)	92.5 (2)	O(8)–Mo(3)–O(20)	164.8 (3)
Br(5)–Mo(1)–O(28)	92.9 (2)	O(12)–Mo(3)–O(16)	165.0 (3)
Br(5)–Mo(1)–O(28)	94.0 (3)	O(12)–Mo(3)–O(20)	79.8 (3)
O(8)–Mo(1)–O(16)	78.5 (3)	O(16)–Mo(3)–O(20)	101.0 (3)
O(8)–Mo(1)–O(28)	81.8 (3)	Mo(1)–Mo(4)–Mo(2)	80.9 (1)
O(8)–Mo(1)–O(32)	170.5 (3)	Mo(1)–Mo(4)–Mo(3)	59.6 (0)
O(16)–Mo(1)–O(28)	160.0 (3)	Mo(1)–Mo(4)–O(8)	53.4 (2)
O(16)–Mo(1)–O(32)	99.4 (3)	Mo(1)–Mo(4)–O(12)	111.4 (2)
O(28)–Mo(1)–O(32)	99.4 (3)	Mo(1)–Mo(4)–O(24)	110.2 (2)
Mo(3)–Mo(2)–Mo(4)	59.5 (0)	Mo(1)–Mo(4)–O(28)	50.9 (2)
Mo(3)–Mo(2)–Br(6)	134.6 (1)	Mo(1)–Mo(4)–O(40)	136.2 (3)
Mo(3)–Mo(2)–O(12)	53.5 (2)	Mo(2)–Mo(4)–Mo(3)	59.6 (0)
Mo(3)–Mo(2)–O(20)	52.9 (2)	Mo(2)–Mo(4)–O(8)	110.4 (2)
Mo(3)–Mo(2)–O(24)	111.2 (2)	Mo(2)–Mo(4)–O(12)	54.2 (2)
Mo(3)–Mo(2)–O(36)	118.3 (3)	Mo(2)–Mo(4)–O(24)	50.9 (2)
Mo(4)–Mo(2)–Br(6)	130.8 (1)	Mo(2)–Mo(4)–O(28)	110.3 (2)
Mo(4)–Mo(2)–O(12)	53.9 (2)	Mo(2)–Mo(4)–O(40)	140.1 (3)
Mo(4)–Mo(2)–O(20)	111.9 (2)	Mo(3)–Mo(4)–O(8)	52.8 (2)
Mo(4)–Mo(2)–O(24)	51.9 (2)	Mo(3)–Mo(4)–O(12)	53.6 (2)
Mo(4)–Mo(2)–O(36)	121.1 (3)	Mo(3)–Mo(4)–O(24)	110.3 (2)
Br(6)–Mo(2)–O(12)	94.5 (2)	Mo(3)–Mo(4)–O(28)	110.3 (2)
Br(6)–Mo(2)–O(20)	94.3 (2)	Mo(3)–Mo(4)–O(40)	119.8 (3)
Br(6)–Mo(2)–O(24)	91.1 (2)	O(8)–Mo(4)–O(12)	93.9 (3)
Br(6)–Mo(2)–O(36)	93.8 (2)	O(8)–Mo(4)–O(24)	159.7 (3)
O(12)–Mo(2)–O(20)	79.3 (3)	O(8)–Mo(4)–O(28)	80.8 (3)
O(12)–Mo(2)–O(24)	81.4 (3)	O(8)–Mo(4)–O(40)	89.8 (3)
O(12)–Mo(2)–O(36)	171.4 (3)	O(12)–Mo(4)–O(24)	81.0 (3)
O(20)–Mo(2)–O(24)	160.2 (3)	O(12)–Mo(4)–O(28)	160.8 (3)
O(20)–Mo(2)–O(36)	97.8 (4)	O(12)–Mo(4)–O(40)	91.8 (3)
O(24)–Mo(2)–O(36)	100.8 (4)	O(24)–Mo(4)–O(28)	97.6 (3)
Mo(1)–Mo(3)–Mo(2)	82.1 (0)	O(24)–Mo(4)–O(40)	109.9 (4)
Mo(1)–Mo(3)–Mo(4)	60.7 (0)	O(28)–Mo(4)–O(40)	106.6 (3)
Mo(1)–Mo(3)–Br(7)	138.7 (1)	Mo(1)–O(8)–Mo(3)	72.7 (2)
Mo(1)–Mo(3)–O(8)	54.3 (2)	Mo(1)–O(8)–Mo(4)	72.6 (2)
Mo(1)–Mo(3)–O(12)	113.6 (2)	Mo(3)–O(8)–Mo(4)	72.4 (6)
Mo(1)–Mo(3)–O(16)	52.1 (2)	Mo(2)–O(12)–Mo(3)	71.5 (2)
Mo(1)–Mo(3)–O(20)	113.6 (2)	Mo(2)–O(12)–Mo(4)	72.0 (2)
Mo(2)–Mo(3)–Mo(4)	60.9 (0)	Mo(3)–O(12)–Mo(4)	71.6 (2)
Mo(2)–Mo(3)–Br(7)	138.6 (1)	Mo(1)–O(16)–Mo(3)	75.1 (3)
Mo(2)–Mo(3)–O(8)	113.7 (2)	Mo(2)–O(20)–Mo(3)	74.9 (2)
Mo(2)–Mo(3)–O(12)	55.0 (2)	Mo(2)–O(24)–Mo(4)	77.1 (3)
Mo(2)–Mo(3)–O(16)	113.6 (2)	Mo(1)–O(28)–Mo(4)	77.3 (3)

Table X. Selected Bond Distances (Å) for the $Mo_4Br_4(O\text{-}i\text{-}Pr)_8$ Molecule

Mo(1)–Mo(2)	2.513 (1)	Mo(2)–Mo(2)′	2.481 (1)
Mo(1)–Mo(2)	2.516 (1)	Mo(2)–Br(4)	2.568 (1)
Mo(1)–Br(3)	2.596 (1)	Mo(2)–O(9)	2.140 (4)
Mo(1)–O(5)	1.843 (4)	Mo(2)′–O(9)	2.150 (4)
Mo(1)–O(9)	2.158 (4)	Mo(2)–O(13)	2.046 (4)
Mo(1)–O(13)	2.020 (4)	Mo(2)–O(17)	2.029 (4)
Mo(1)–O(17)	2.022 (4)		

of the molecule is shown in Figure 3. A space-filling model of the same view of the molecule is also given in Figure 3.

The molecule has crystallographically imposed C_2 and virtual C_{2v} symmetry and can be seen to be closely related to its precursor $Mo_4Br_3(O\text{-}i\text{-}Pr)_9$ by replacement of the terminal Mo–O-*i*-Pr bond on the Mo_4 backbone by a Mo–Br bond. The Mo–Mo, Mo–Br, and Mo–O (μ_3, μ_2, and terminal) distances are very similar to those in $Mo_4Br_3(O\text{-}i\text{-}Pr)_9$.

$Mo_4Cl_4(O\text{-}i\text{-}Pr)_8$. A ball and stick drawing of this molecule is given in Figure 4 along with a corresponding space-filling drawing. The molecule has virtual D_{4h} and crystallographically

Table XI. Selected Bond Angles (deg) for the $Mo_4Br_4(O\text{-}i\text{-}Pr)_8$ Molecule

Mo(2)–Mo(1)–Mo(2)′	59.1 (0)	Mo(1)–Mo(2)–Br(4)	137.1 (0)
Mo(2)–Mo(1)–Br(3)	132.3 (0)	Mo(1)–Mo(2)–O(9)	112.9 (1)
Mo(2)–Mo(1)–O(5)	118.6 (1)	Mo(1)–Mo(2)–O(13)	112.9 (1)
Mo(2)–Mo(1)–O(9)	54.2 (1)	Mo(1)–Mo(2)–O(17)	113.3 (1)
Mo(2)–Mo(1)–O(13)	52.2 (1)	Mo(2)–Mo(2)′–Br(6)	118.9 (0)
Mo(2)–Mo(1)–O(17)	51.8 (1)	Mo(2)–Mo(2)′–O(9)	54.9 (1)
Br(3)–Mo(1)–O(5)	93.6 (1)	Mo(2)–Mo(2)′–O(13)	111.2 (1)
Br(3)–Mo(1)–O(9)	94.9 (1)	Mo(2)–Mo(2)′–O(17)	111.4 (1)
Br(3)–Mo(1)–O(13)	94.1 (1)	Br(4)–Mo(2)–O(9)	89.7 (1)
Br(3)–Mo(1)–O(17)	90.7 (1)	Br(4)–Mo(2)–O(13)	106.7 (1)
O(5)–Mo(1)–O(9)	171.5 (2)	Br(4)–Mo(2)–O(17)	105.2 (1)
O(5)–Mo(1)–O(13)	99.9 (2)	O(9)–Mo(2)–O(9)′	96.3 (2)
O(5)–Mo(1)–O(17)	102.0 (2)	O(9)–Mo(2)–O(13)	78.5 (2)
O(9)–Mo(1)–O(13)	78.6 (2)	O(9)–Mo(2)–O(17)	78.7 (2)
O(9)–Mo(1)–O(17)	78.7 (2)	O(13)–Mo(2)–O(17)	102.0 (2)
O(13)–Mo(1)–O(17)	157.2 (2)	Mo(1)–O(9)–Mo(2)	71.4 (1)
Mo(1)–Mo(2)–Mo(1)′	81.6 (0)	Mo(2)–O(9)–Mo(2)′	70.7 (1)
Mo(1)–Mo(2)–Mo(2)′	60.4 (0)	Mo(2)–O(13)–Mo(2)′	70.7 (1)

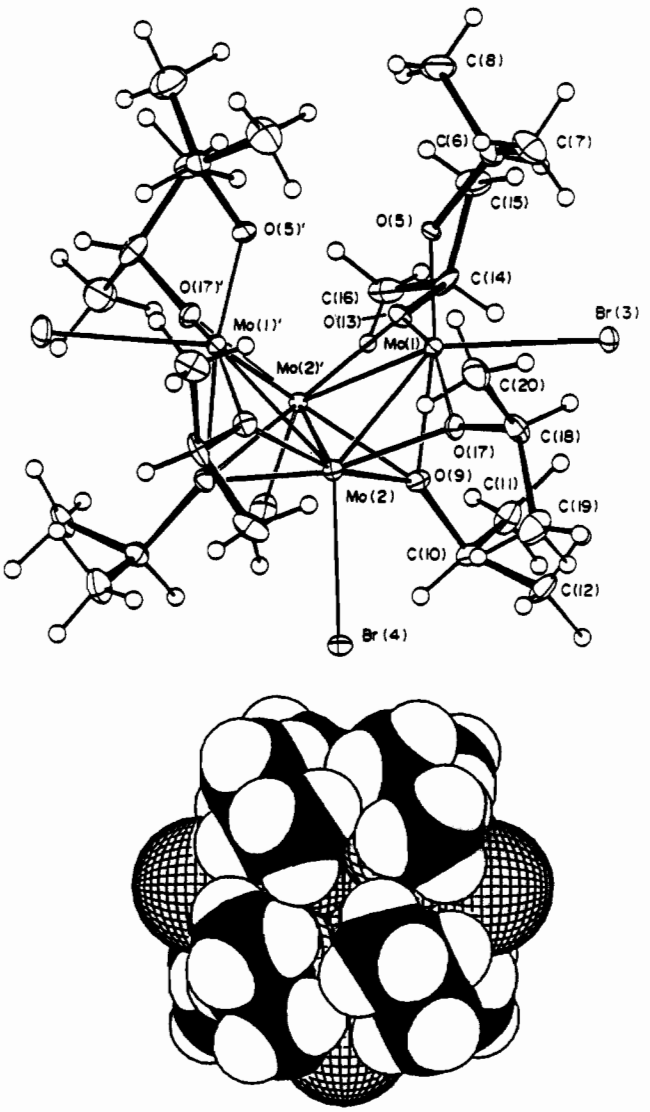

Figure 3. ORTEP view of the $Mo_4Br_4(O\text{-}i\text{-}Pr)_8$ molecule parallel to the mirror plane bisecting the backbone of the Mo_4 butterfly unit, giving the atom-numbering scheme used in the tables. A space-filling model diagram of the same view is shown at the bottom.

imposed C_{2h} symmetry. There is a square Mo_4 unit with Mo–Mo = 2.38 Å (average) with eight bridging (μ_2) O-*i*-Pr ligands, four above and four below the Mo_4 plane. The terminal Mo–Cl bonds radiate from the center of the Mo_4 square, and the local MoO_4Cl units are square pyramidal with the Mo–Cl bonds in the apical position. Selected bond distances and angles are given in Table XII.

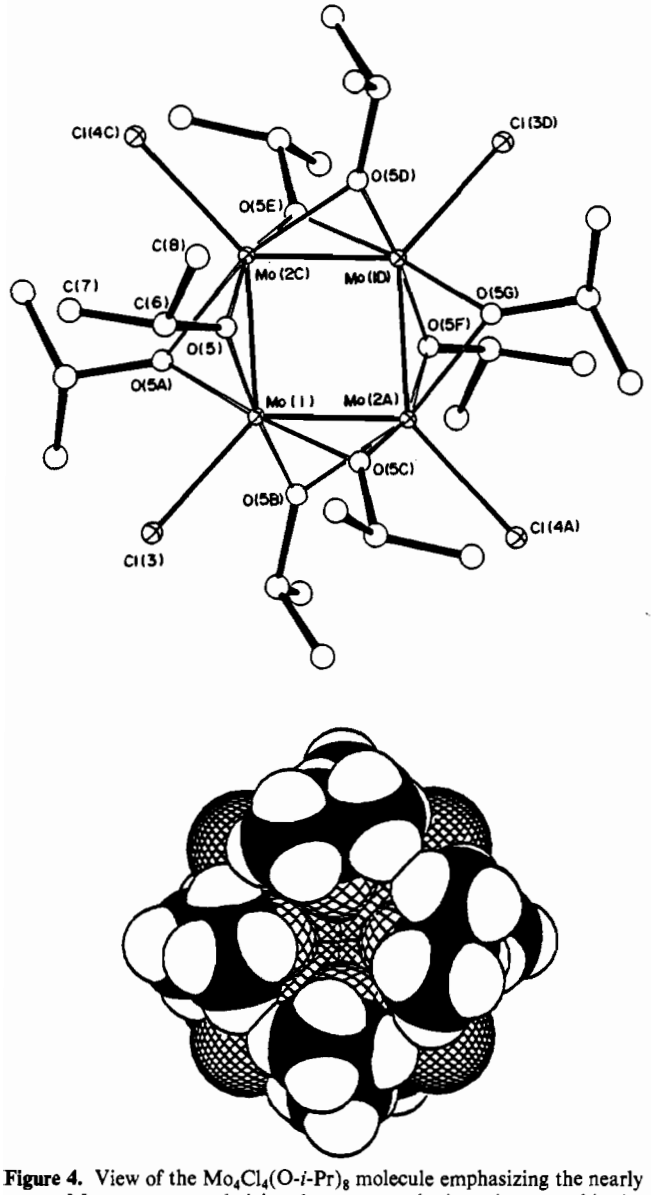

Figure 4. View of the $Mo_4Cl_4(O\text{-}i\text{-}Pr)_8$ molecule emphasizing the nearly square Mo_4 geometry and giving the atom-numbering scheme used in the tables. The molecule has a crystallographically imposed C_2 axis, which contains Cl(3)–Mo(1)–Mo(1D)–Cl(3D), and a mirror plane, which contains Cl(4C)–Mo(2C)–Mo(2A)–Cl(4A) and relates atoms O(5) and O(5D), O(5A) and O(5E), etc. A space-filling model diagram of the same view is shown at the bottom.

Table XII. Selected Bond Distances (Å) and Bond Angles (deg) for the $Mo_4Cl_4(O\text{-}i\text{-}Pr)_8$ Molecule

Mo(1)–Mo(2)	2.378 (2)	Mo(2)–Cl(4)	2.432 (5)
Mo(1)–Cl(3)	2.442 (5)	Mo(2)′–O(5)′	2.078 (4)
Mo(1)–O(5)	1.981 (4)	Mo(4)–O(5)	2.138 (5)
Mo(2)–Mo(2)′	2.407 (3)		
Mo(2)–Mo(1)–Mo(2)′	91.4 (1)	Mo(1)–Mo(2)–O(5)	51.7 (1)
Mo(2)–Mo(1)–Cl(3)	134.3 (1)	Mo(2)–Mo(1)–Mo(2)′	91.4 (1)
Mo(2)–Mo(1)–O(5)	56.1 (1)	Mo(2)–Mo(1)′–Mo(2)′	90.0 (0)
Cl(3)–Mo(1)–O(5)	93.3 (1)	Mo(2)–Mo(2)′–Cl(4)	139.6 (1)
O(5)–Mo(1)–O(5)′	89.8 (0)	Mo(2)–Mo(2)′–O(5)	54.0 (1)
Mo(1)–Mo(2)–Mo(1)′	88.6 (1)	Cl(4)–Mo(2)–O(5)	102.3 (1)
Mo(1)–Mo(2)–Mo(2)′	59.6 (0)	O(5)–Mo(2)–O(5)′	83.1 (2)
Mo(1)–Mo(2)–Cl(4)	135.5 (1)	Mo(1)–O(5)–Mo(2)	70.4 (1)

Spectroscopic Studies

NMR Studies. $Mo_4F_2(O\text{-}i\text{-}Pr)_{10}$ is thermally unstable in toluene-d_8 at ambient temperatures and very sparingly soluble at low temperatures, which makes its detailed study by NMR spectroscopy difficult. In the temperature range 0–20 °C only broad resonances are seen in the ^1H NMR spectra, implying a dynamic process that is rapid on the NMR time scale. At −40 °C, however, there are six methyne resonances as shown in Figure 5. For a molecule having C_{2h} symmetry (Figure 1) three methyne resonances are expected in the integral ratio 2:2:1 corresponding to the two types of terminal O-*i*-Pr ligands (2:2) and the bridging O-*i*-Pr ligands, respectively. From the appearance of the spectrum it is clear that there are in fact two sets of resonances, each having a 2:2:1 integral ratio. We conclude that in toluene-d_8 $Mo_4F_2(O\text{-}i\text{-}Pr)_{10}$ exists as a mixture of isomers of roughly 2:1 relative concentration. The downfield methyne resonances are unusually deshielded for O-*i*-Pr ligands. Their relative integral intensity determines that they must be terminal O-*i*-Pr ligands, and it is reasonable to assign these to O-*i*-Pr ligands that are cis to the fluoride bridges.[16] The isomers in solution must either have a C_2 axis of symmetry or be centrosymmetric. This can be accommodated by a compound of formula $[Mo_2(\mu\text{-}F)(\mu\text{-}O\text{-}i\text{-}Pr)(O\text{-}i\text{-}Pr)_2]_2$ having either a Mo_4 bisphenoid or a Mo_4 rectangle. The Mo_4 bisphenoid would be a variation of the structure seen for $Mo_4F_4(O\text{-}t\text{-}Bu)_8$, **1**, in which two opposite bridging fluoride ligands were replaced by OR groups. The possible rectangular Mo_4 geometries are shown in **2a** and **2b**, where **2a** represents the structure observed in the solid state.

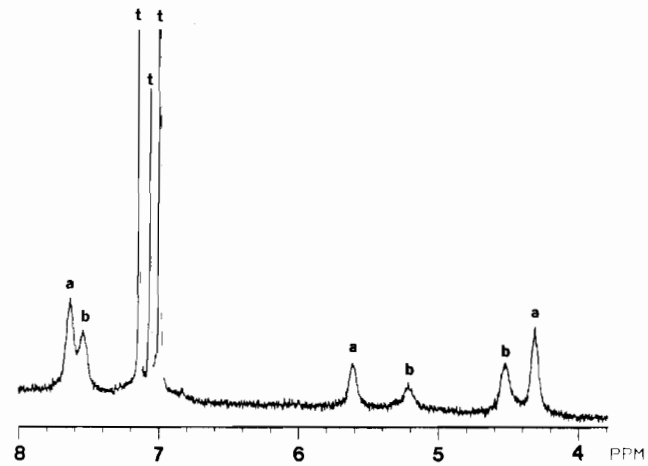

Figure 5. 360-MHz ^1H NMR spectrum of $Mo_4F_2(O\text{-}i\text{-}Pr)_{10}$ in toluene-d_8 solution at −40 °C. Only the methyne region of the spectrum is shown. Those peaks marked "t" arise from the ^1H impurity of toluene-d_8.

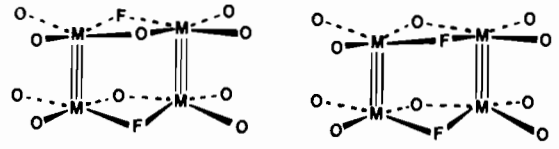

2a **2b**

It is important to recognize that the observed dynamic nature of $Mo_4F_2(O\text{-}i\text{-}Pr)_{10}$ implies that bridges must be opening and closing rapidly on the NMR time scale. Undoubtedly this is responsible for its facile disproportionation and reactivity toward PMe_3 to give $Mo_2(O\text{-}i\text{-}Pr)_6$ and $Mo_2F_2(O\text{-}i\text{-}Pr)_4(PMe_3)_2$.

$Mo_2F_2(O\text{-}i\text{-}Pr)_4(PMe_3)_2$ shows two types of O-*i*-Pr ligands, each having diastereotopic isopropyl methyl groups in the ^1H NMR spectrum. There is by ^{19}F and $^{31}P\{^1H\}$ NMR spectroscopy a single type of fluoride and phosphide ligand, and their spectra comprise an AA′XX′ spin system as previously discussed for $Mo_2F_2(O\text{-}t\text{-}Bu)_4(PMe_3)_2$.[6]

$Mo_2Cl_2(O\text{-}i\text{-}Pr)_4(PMe_2(O\text{-}i\text{-}Pr))_2$ shows three types of O-*i*-Pr ligands, each having diastereotopic methyl groups, and a single type of phosphine ligand whose PMe_2 groups are also diastereotopic. The NMR data are given in the Experimental Section, and collectively they unequivocally identify the compounds $Mo_2F_2(O\text{-}i\text{-}Pr)_4(PMe_3)_2$ and $Mo_2Cl_2(O\text{-}i\text{-}Pr)_4(PMe_2(O\text{-}i\text{-}Pr))_2$ as ana-

(16) A similar deshielding was seen in the spectra of $Mo_2X_4(O\text{-}i\text{-}Pr)_6$ compounds (X = Cl, Br, and I) for the methyne protons which were in close proximity to the halides: Chisholm, M. H.; Kirkpatrick, C. C.; Huffman, J. C. *Inorg. Chem.* **1981**, *20*, 871.

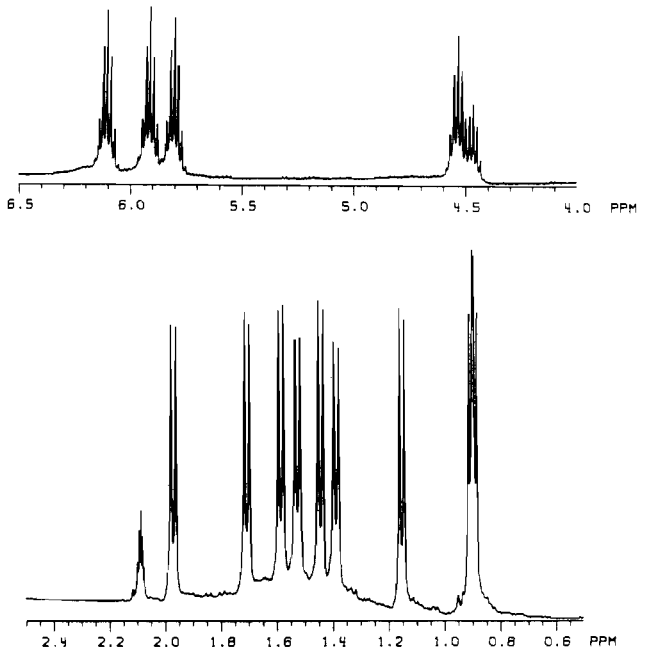

Figure 6. Methyne (top) and methyl (bottom) portions of the ^1H NMR spectrum of $Mo_4Cl_3(O\text{-}i\text{-}Pr)_9$ in toluene-d_8 solution at 22 °C and 360 MHz. The resonance at 2.09 ppm is due to the ^1H impurity in toluene-d_8.

logues of the structurally characterized compound $Mo_2F_2(O\text{-}t\text{-}Bu)_4(PMe_3)_2$[6] having two four-coordinate metal atoms with cis-OR groups united by a M≡M bond about which rotation is rapid on the NMR time scale.

$Mo_4X_3(O\text{-}i\text{-}Pr)_9$ compounds, where X = Cl, Br, and I, show quite remarkable ^1H NMR spectra: there are five methyne septets in the integral ratio 2:2:2:2:1 and nine partially overlapping doublets of equal intensity for the methyl groups. The spectrum of the chloro compound is shown in Figure 6. The spectra are invariant in the temperature range +60° to −60 °C in toluene-d_8, implying a nonfluxional molecule. The spectra are consistent with expectations based on the observed solid-state molecular structure of $Mo_4Br_3(O\text{-}i\text{-}Pr)_9$, which has a mirror plane of symmetry containing the Mo–Mo backbone thereby relating the two wingtip Mo atoms and their attendant ligands. There are a symmetry-related pair of μ_3-O-*i*-Pr ligands, two pairs of μ_2-O-*i*-Pr ligands, a pair of terminal O-*i*-Pr ligands, and a unique O-*i*-Pr group attached to a backbone Mo atom. The last type, but none of the first three types, lies on a mirror plane, which means that only the O-*i*-Pr ligand attached to the backbone contains nondiastereotopic isopropyl methyl groups.

$Mo_4X_4(O\text{-}i\text{-}Pr)_8$ compounds, where X = Cl, Br, and I, show very similar ^1H NMR spectra, again implying a similar solution structure and solution behavior, though the chloro compound is only very sparingly soluble. At 22 °C, there are three very broad signals in the methyne region and four very broad resonances in the isopropyl region. When the temperature is raised, the resonances broaden further but a fast-exchange limiting spectrum cannot be reached because the compounds react to form $Mo_4O_2X_2(O\text{-}i\text{-}Pr)_6$ compounds with elimination of 2 equiv of *i*-PrX (eq 8). When the temperature is lowered to −40 °C in toluene-d_8, a low-temperature limiting spectrum is achieved for each compound. The spectrum of the bromo compound is shown in Figure 7.

The low-temperature limiting ^1H NMR spectrum shows three types of methyne resonances in the integral ratio 2:1:1 and four doublets in the methyl region of equal intensity. This is consistent with the observed solid-state molecular structure found for $Mo_4Br_4(O\text{-}i\text{-}Pr)_8$ (Figure 3), which has virtual C_{2v} symmetry. There are four equivalent μ_2-O-*i*-Pr ligands that have diastereotopic methyl groups and two pairs of O-*i*-Pr ligands (μ_3 and terminal) that lie on molecular planes of symmetry. There are in addition some other minor resonances in the low-temperature spectra of $Mo_4X_4(O\text{-}i\text{-}Pr)_8$ compounds, some of which can be

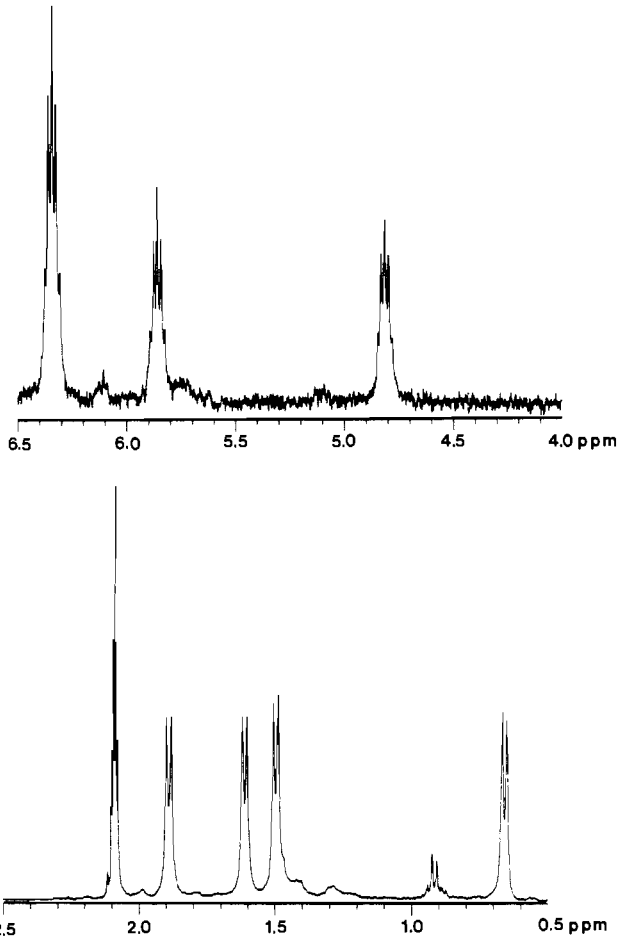

Figure 7. Methyne (top) and methyl (bottom) portions of the low-temperature limiting ^1H NMR spectrum of $Mo_4Br_4(O\text{-}i\text{-}Pr)_8$ in toluene-d_8 solution at −40 °C and 360 MHz. The resoannce at 2.09 ppm is due to the ^1H impurity in toluene-d_8.

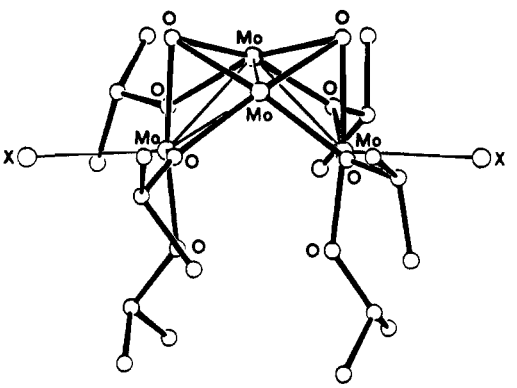

Figure 8. View of the proposed structure of the $Mo_4O_2X_2(O\text{-}i\text{-}Pr)_6$ molecule.

traced to $Mo_4X_3(O\text{-}i\text{-}Pr)_9$ and $Mo_4O_2X_2(O\text{-}i\text{-}Pr)_6$ impurities. The signals due to the impurities account for less than 5% of the signals assignable to $Mo_4X_4(O\text{-}i\text{-}Pr)_8$ above. However, it is just possible that another isomer might be present in solution. The observed line broadening at room temperature is not due to exchange with free *i*-PrOH, nor do the spectra change as a function of concentration. Thus, we propose that the line broadening arises from O-*i*-Pr group scrambling in an intramolecular manner. This is, of course, not uncommon for metal alkoxides;[17] e.g., $W_4(H)_2(O\text{-}i\text{-}Pr)_{14}$, which has seven different types of O-*i*-Pr ligands in the solid state, shows only one time-averaged O-*i*-Pr ligand on the ^1H NMR time scale at −60 °C in toluene-d_8 at 220 MHz.[18]

(17) Bradley, D. C.; Mehrotra, R. C.; Gaur, P. D. In *Metal Alkoxides*; Academic: New York, 1978.

Figure 9. Comparison of the ν(Mo–O) fingerprint region of the IR spectra of (a) $Mo_4Cl_3(O\text{-}i\text{-}Pr)_9$ and (b) $Mo_4Cl_4(O\text{-}i\text{-}Pr)_8$.

$Mo_4O_2X_2(O\text{-}i\text{-}Pr)_6$ compounds (X = Cl, Br, and I) show temperature-invariant (+60 to −60 °C) ^1H NMR spectra in toluene-d_8. There are two types of methyne resonances in the integral ratio 2:1 and three isopropyl methyl doublets of equal intensity. The seemingly most plausible structure for these compounds is based on a Mo_4 butterfly having two capping (μ_3) oxo ligands as shown in Figure 8.

Infrared spectra of the new compounds reported here are recorded in the Experimental Section. As with most metal alkoxides, we find strong bands in the region 900–1100 cm^{-1} assignable to ν(C–O) and several bands in the region 650–500 cm^{-1}, which is typically the region of ν(M–O).[17,19] For the compounds $Mo_2F_2(O\text{-}i\text{-}Pr)_4(PMe_3)_2$ and $Mo_2Cl_2(O\text{-}i\text{-}Pr)_4(PMe_2(O\text{-}i\text{-}Pr))_2$ we can assign ν(Mo–F) = 510 cm^{-1} and ν(Mo–Cl) = 305 cm^{-1}. The spectra of $Mo_4X_3(O\text{-}i\text{-}Pr)_9$ compounds (X = Cl, Br, and I) are virtually identical with the exception of two medium-intensity bands at 287 and 232 cm^{-1} present in the chloride but absent in the iodide and bromide. Again it is reasonable to assign these to ν(Mo–Cl). Similarly for the compound $Mo_4Cl_4(O\text{-}i\text{-}Pr)_8$ two medium-intensity bands near 290 and 230 cm^{-1} may be assigned to ν(Mo–Cl).

The most important aspect of the infrared spectral data is that they may be used to support the different structures of the $Mo_4X_4(O\text{-}i\text{-}Pr)_8$ compounds where X = Cl versus those where X = Br and I. The butterfly Mo_4 clusters display a very distinctive and characteristic pattern in the 650–500-cm^{-1} region of the spectrum. They show six resolved absorptions that serve as a "fingerprint" for the butterfly clusters, similar to the use of combination and overtone absorptions to identify ring substitution patterns of aromatic rings.[20] By contrast, the infrared spectrum of $Mo_4Cl_4(O\text{-}i\text{-}Pr)_8$ shows only four bands in this region. Since the infrared spectra were all recorded as Nujol mulls, this may be taken as further evidence that in the solid state the $Mo_4X_4(O\text{-}i\text{-}Pr)_8$ compounds where X = Br and I adopt a structure different from that of the chloride. A comparison of this "fingerprint" region of the spectrum is shown for $Mo_4Cl_3(O\text{-}i\text{-}Pr)_9$ and $Mo_4Cl_4(O\text{-}i\text{-}Pr)_8$ in Figure 9.

Electronic Absorption Spectra. The room-temperature electronic absorption spectra of I and II show weak (ϵ = 500 M^{-1} cm^{-1}) absorptions in the near-infrared region, three medium-intensity (ϵ = 1000–4000 M^{-1} cm^{-1}) absorptions in the visible region, and one or more very intense (ϵ = 15000–45000 M^{-1} cm^{-1}) absorptions in the ultraviolet region. A representative series of spectra is shown in Figure 10, which compares the three halide derivatives of I.

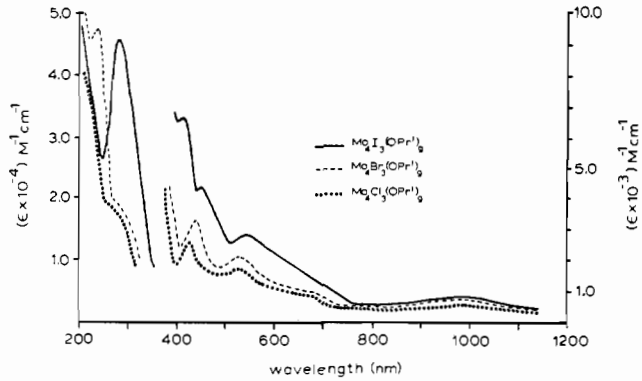

Figure 10. Comparison of the UV–visible electronic absorption spectra of $Mo_4X_3(O\text{-}i\text{-}Pr)_9$ compounds for X = I (solid line), X = Br (dashed line), and X = Cl (dotted line) in hexane solution.

The most prominent feature is the very intense absorption (ϵ = 45000 M^{-1} cm^{-1}) in the ultraviolet region, which shifts to lower energy upon traversing the series from Cl to Br to I. This behavior is typical of halide-to-metal charge-transfer (LMCT) transitions in hexahalo transition-metal complexes. For a given metal ion, the absorption energies decrease in the sequence $MCl_6 > MBr_6 > MI_6$, which is the order of decreasing ionization potentials of the halogen atoms.[21,22] The high-energy transitions of I and II follow the same trend and are reasonably assigned to halide-to-metal charge-transfer (LMCT) transitions at 50000 cm^{-1} (ϵ = 40000 M^{-1} cm^{-1}) for the chloride, 43100 cm^{-1} (ϵ < 48000 M^{-1} cm^{-1}) for the bromide, and 38500 cm^{-1} (ϵ = 44000 M^{-1} cm^{-1}) for the iodide.

Another feature evident in the ultraviolet region of the spectra of both I and II is an intense absorption (ϵ = 15000 M^{-1} cm^{-1}) centered near 260 nm (38500 cm^{-1}), which is invariant to the nature of X. This behavior is consistent with a charge-transfer transition originating from the alkoxide ligands. Transitions of similar energy and intensity have been observed in dinuclear alkoxides such as $Mo_2(OR)_6$[23] and, more importantly, in the alkoxide-supported trinuclear clusters of formulas $M_3(\mu_3\text{-}O)(\mu_3\text{-}OR)(\mu_2\text{-}OR)_3(OR)_6$ (M = Mo, W).[24,25] A comparison of Mo_3 and W_3 clusters showed a shift of these transitions to higher energy by 0.7 eV for the W_3 cluster, with the mixed-metal Mo_2W cluster exhibiting a transition at intermediate energy.[25] Since the W_3 complex was found to be 0.7 V harder to reduce electrochemically than the Mo_3 cluster, the observed shift in absorbance is exactly that expected for an oxygen-to-metal LMCT transition. In view of the energetics, intensity, and invariance upon change of X, the tentative assignment of an oxygen-to-metal LMCT transition at 38500 cm^{-1} seems very reasonable for the Mo_4 butterfly clusters as well.

The other interesting feature is the weak absorption (ϵ = 500 M^{-1} cm^{-1}) in the near-infrared region of the spectra that is present for all the Mo_4 butterfly clusters. The low energy and low intensity of these absorptions are suggestive of transitions between metal-centered molecular orbitals in a fashion similar to that observed in the triangular clusters $M_3(\mu_3\text{-}O)(\mu_3\text{-}OR)(\mu\text{-}OR)_3(OR)_6$ (M = Mo and W). This suggestion is supported by Fenske–Hall molecular orbital calculations, which predict the HOMO to be a metal-based orbital of a_1 symmetry that is delocalized across the backbone of the butterfly.[26] The LUMO is predicted to be its antibonding b_1 counterpart, and the HOMO–LUMO gap is calculated to be rather small, ca. 1.8 eV (14500 cm^{-1}). The lowest energy transition seen for all the Mo_4 butterfly clusters is centered

(18) Akiyama, M.; Chisholm, M. H.; Cotton, F. A.; Extine, M. W.; Haitko, D. A.; Leonelli, J.; Little, D. *J. Am. Chem. Soc.* **1981**, *103*, 779.
(19) Bradley, D. C. *Proc. Symp. Coord. Chem.* **1965**, 1964.
(20) Pavia, D. L.; Lampman, G. M.; Kriz, G. S., Jr. In *Introduction to Spectroscopy: A Guide for Students of Organic Chemistry*; Saunders: Philadelphia, 1979.
(21) Jørgensen, C. K. *Mol. Phys.* **1959**, *2*, 309.
(22) Jørgensen, C. K. *Adv. Chem. Phys.* **1963**, *5*, 33.
(23) Chisholm, M. H.; Clark, D. L.; Kober, E. M.; Van Der Sluys, W. G. *Polyhedron* **1987**, *6*, 723.
(24) Chisholm, M. H.; Cotton, F. A.; Fang, A.; Kober, E. M. *Inorg. Chem.* **1984**, *23*, 749.
(25) Chisholm, M. H.; Folting, K.; Huffman, J. C.; Kober, E. M. *Inorg. Chem.* **1985**, *24*, 241.
(26) Bursten, B. E.; Chisholm, M. H.; Clark, D. L. *Inorg. Chem.*, following paper in this issue.

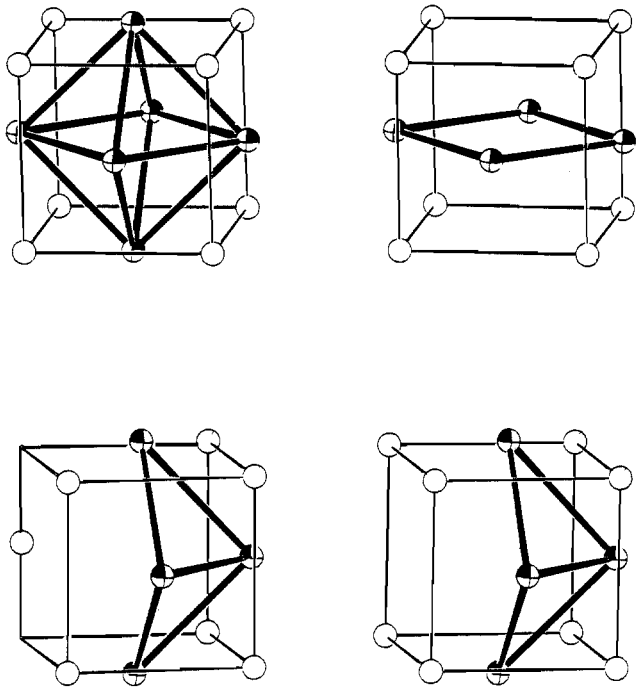

Figure 11. Cube–octahedral relationship found in the *closo*-$Mo_6(\mu_3\text{-}X)_8^{4+}$ compounds (top left), the *arachno*-Mo_4O_8 moiety in $Mo_4Cl_4(O\text{-}i\text{-}Pr)_8$ (top right), the *arachno*-Mo_4O_8 moiety in $Mo_4Br_4(O\text{-}i\text{-}Pr)_8$ (bottom right), and the *arachno*-$Mo_4I_7^{2+}$ moiety in $Mo_4I_{11}^{2-}$ (bottom left).

near 10 000 cm^{-1} (1000 nm) and is tentatively assigned to the allowed singlet ($A_1 \rightarrow B_1$) HOMO → LUMO transition. The low intensity of these transitions presumably results from the predominant d-orbital character of these molecular orbitals.

Structural Similarities between Square and Butterfly Mo_4 Clusters: Cube–Octahedral Relationships and the Radial Cluster Influence. Why does $Mo_4Cl_4(O\text{-}i\text{-}Pr)_8$ adopt a square Mo_4 structure whereas the related bromo and iodo compounds, and even the immediate precursor $Mo_4Cl_3(O\text{-}i\text{-}Pr)_9$, adopt Mo_4 butterfly structures? The only logical answer to this question is that the total energies of the square and butterfly molecules are very similar and packing forces are sufficient to favor the square Mo_4 geometry in the solid state for $Mo_4Cl_4(O\text{-}i\text{-}Pr)_8$. At first this might seem surprising, but, though the $Mo_4X_4(O\text{-}i\text{-}Pr)_8$ structures (X = Cl, Br) appear very different, they are in fact very closely related to one another. Both contain Mo_4 units within a cube of O ligands and as such can be viewed as arachno fragments of the well-known $Mo_6(\mu_3\text{-}X)_8^{4+}$ unit.[27-29] The $Mo_6(\mu_3\text{-}X)_8^{4+}$ unit is shown in the upper left corner of Figure 11 and consists of an octahedron of Mo atoms within a cube of X ligands. Terminal ligands radiate from the faces of the X_8 cube, or when the structure is viewed in another way, terminal ligands radiate from the vertices of the Mo_6 octahedron. By removal of two opposite Mo vertices, one obtains the structure of the Mo_4 square cluster that can be viewed as an arachno derivative of the closo Mo_6 octahedron. The alkoxy ligands in the arachno Mo_4 square derivative are all doubly bridging, and the halides radiate from the Mo vertices. In a similar fashion, removal of two adjacent Mo vertices from the Mo_6 octahedron yields the structure of the Mo_4 butterfly shown in the lower right corner of Figure 11, which is an alternate arachno derivative of the Mo_6 octahedron. This readily accounts for two triply bridging, four doubly bridging, and two terminal alkoxides while the halides again radiate from the Mo vertices. The butterfly structure may also be compared with the $Mo_4I_{11}^{2-}$ structure reported by McCarley and co-workers.[30] The latter also contains a butterfly Mo_4 core and may also be viewed as a derivative of the $Mo_6(\mu_3\text{-}X)_8^{4+}$ core: the central $Mo_4I_7^{2+}$ core contains six I^- ligands at the corners of the cube, while the seventh bridges the two wingtip molybdenum atoms at the midpoint of the edge of the idealized I_8 cube as shown in the lower left corner of Figure 11.

Only recently, McCarley and Aufdembrink reported[31] the discovery of a new chloromolybdate ion of formula $Mo_4Cl_{12}^{3-}$. Quite remarkably, this ion adopts either a rectangular or a butterfly Mo_4 geometry in the solid state depending on the nature of the countercation. The rectangular and butterfly Mo_4 cluster units are hauntingly familiar and may also be viewed as arachno subunits of the *closo*-$Mo_6(\mu_3\text{-}X)_8^{4+}$ cluster unit. This new chloromolybdate anion provides yet another striking example of extremely subtle factors favoring one arachno Mo_4 subunit of the Mo_6 octahedron over another in the solid state.

Having recognized that the square and butterfly Mo_4 clusters can be viewed as arachno subunits of a closo Mo_6 octahedral cluster, we note that the radial halide ligands all have abnormally long Mo–X distances. To appreciate this, one must obtain a reliable estimate for normal Mo(III)–X distances. A reliable estimate for the single-bond covalent radius of Mo(III) has previously been established to be 1.40 Å.[15,32] The single-bond covalent radius for chlorine is 0.99 Å,[33] and this allows for an estimate of $d_{Mo-Cl} = r_{Mo} + r_{Cl} = 2.39$ Å. This value is in fact very close to the observed terminal Mo(III)–Cl distance of 2.35 Å found for $Mo_2Cl_2(NMe_2)_4$[13,34] but considerably shorter than the terminal Mo–Cl distance of 2.44 Å found in $Mo_4Cl_4(O\text{-}i\text{-}Pr)_8$. In an analogous fashion, the single-bond covalent radius of bromine is known to be 1.14 Å,[33] which places $d_{Mo-Br} = r_{Mo} + r_{Br} = 2.54$ Å. This value is close to that observed for $W_2Br_2(NEt_2)_4$, 2.48 Å,[35] but notably shorter than the terminal Mo–Br bonds in $Mo_4Br_3(O\text{-}i\text{-}Pr)_9$ and $Mo_4Br_4(O\text{-}i\text{-}Pr)_8$, which average 2.60 Å. It is also noteworthy that, in $Mo_4Br_3(O\text{-}i\text{-}Pr)_9$, the unique alkoxide on the backbone of the butterfly occupies a radial position and is ca. 0.1 Å longer than the other two terminal alkoxides, which show an average terminal Mo–O distance of 1.86 Å.

These long Mo–X bond distances for radial ligands can, in principle, be traced all the way back to the closo Mo_6 cluster. During structural studies of octahedral Mo_6 clusters supported by methoxide ligands, Chisholm, Heppert, and Huffman noted[36] a substantial lengthening of radial Mo–X bonds with the μ_3-X ligand. For example, substitution of μ_3-Cl ligands in $Mo_6(\mu_3\text{-}Cl)_8(OMe)_6^{2-}$ by μ_3-OMe ligands to yield $Mo_6(\mu_3\text{-}OMe)_8(OMe)_6^{2-}$ resulted in a substantial shortening (from 2.61 to 2.54 Å) in the Mo–Mo distances with concomitant lengthening in the radial Mo–O distances by close to 0.1 Å.[36] We propose that electronic factors are responsible for the long radial Mo–X bonds in the alkoxide-supported Mo_4 and Mo_6 clusters. Each molybdenum atom forms a square-based pyramid with radial ligands occupying apical coordination sites. If one defines the atomic z axis to be coincident with the radial Mo–X bonds, then there will be a competition for use of molybdenum valence s, p_z, and d_{z^2} atomic orbitals for σ-bonding between strong metal–metal cluster bonding and metal–ligand bonding in the radial position. This competition for σ-bonding represents a mutual trans influence,[37] and its effect on the radial Mo–Br bonds (2.60 Å) can be compared to the trans influence of the trans =CHSiMe$_3$ ligands on the Mo–Br bonds

(27) Schafer, H.; von Schneering, H. G. *Angew. Chem.* **1971**, *385*, 75.
(28) Guggenberger, L. J.; Sleight, A. W. *Inorg. Chem.* **1969**, *8*, 2041.
(29) Healy, P. C.; Kepert, D. L.; Taylor, D.; White, A. W. *J. Chem. Soc., Dalton Trans.* **1973**, 646.
(30) Stensvad, S.; Helland, B. J.; Babich, M. W.; Johnson, R. A.; McCarley, R. E. *J. Am. Chem. Soc.* **1978**, *100*, 6257.
(31) Aufdembrink, B. A.; McCarley, R. E. *J. Am. Chem. Soc.* **1986**, *108*, 2474.
(32) Chisholm, M. H.; Corning, J. F.; Folting, K.; Huffman, J. C. *Polyhedron* **1985**, *4*, 383.
(33) Pauling, L. *The Nature of the Chemical Bond*; Cornell University Press: New York, 1960; Table 7.2, p 224.
(34) See also W–X distances in $W_2X_2(NEt_2)_4$ compounds, where X = Cl, Br, and I: Chisholm, M. H.; Cotton, F. A.; Extine, M. W.; Millar, M.; Stults, B. R. *Inorg. Chem.* **1977**, *16*, 320.
(35) Chisholm, M. H.; Cotton, F. A.; Extine, M. W.; Millar, M.; Stults, B. R. *Inorg. Chem.* **1977**, *16*, 320.
(36) Chisholm, M. H.; Heppert, J. A.; Huffman, J. C. *Polyhedron* **1984**, *3*, 475.
(37) Appleton, T. G.; Clark, H. C.; Manzer, L. M. *Coord. Chem. Rev.* **1972**, *10*, 335.

(2.64 Å) in $Mo_2Br_2(=CHSiMe_3)_2(PMe_3)_4$.[38] We shall refer to this competition of σ-bonding between metal–metal cluster and radial metal–ligand bonding as a *radial cluster influence*.[26]

Clearly, a more quantitative examination of the electronic structure and bonding in the square and butterfly clusters is warranted, and this will be discussed in the following paper.

Concluding Remarks

Substitution of halide for isopropoxide has provided a successful route to tetranuclear Mo_4 clusters starting from the M≡M-bonded $Mo_2(O\text{-}i\text{-}Pr)_6$ compounds. The coupling of $Mo_2X(O\text{-}i\text{-}Pr)_5$ or $Mo_2X_2(O\text{-}i\text{-}Pr)_4$ units is dependent on the nature of X. When X = F, the initial coupling involves two $Mo_2F(O\text{-}i\text{-}Pr)_5$ molecules to give $Mo_4F_2(O\text{-}i\text{-}Pr)_{10}$. When X = Cl, Br, or I, the coupling involves $Mo_2X(O\text{-}i\text{-}Pr)_5$ with $Mo_2X_2(O\text{-}i\text{-}Pr)_4$. There are obviously subtle electronic and steric factors at work here since for reactions employing $Mo_2(O\text{-}t\text{-}Bu)_6$ with PF_3 the tetranuclear compound $Mo_4F_4(O\text{-}t\text{-}Bu)_8$ is formed by the dimerization of two $Mo_2F_2(O\text{-}t\text{-}Bu)_4$ units.

It seems likely that in all of the coupling reactions there is initial halide bridge formation. In the case of fluoride compounds these are kinetically inert to cluster formation, whereas for X = Cl, Br, and I the initially formed halide-bridged complexes rearrange to 12-electron Mo_4 clusters. The difference between the fluoro and the other halide complexes is quite striking and may well reflect the flexibility of the M–X–M angle. There is, of course, considerable uncertainty as to the detailed pathway of association and the reason for the apparent reluctance of the fluoro derivatives to form clusters.

The $Mo_4X_3(O\text{-}i\text{-}Pr)_9$ and $Mo_4X_4(O\text{-}i\text{-}Pr)_8$ compounds (X = Cl, Br, and I) all favor a Mo_4 butterfly geometry in solution, and apparently, with one exception, $Mo_4Cl_4(O\text{-}i\text{-}Pr)_8$, these are also found in the solid state. However, the observations that this last compound adopts a square Mo_4 structure in the solid state and that all $Mo_4X_4(O\text{-}i\text{-}Pr)_8$ compounds (X = Cl, Br, and I) show fluxional behavior in solution (O-*i*-Pr group scrambling) lead us to conclude that (i) these square and butterfly Mo_4 12-electron clusters must have very similar total energies and (ii) their interconversion must be chemically facile such that the fluxional solution behavior of the alkoxide ligands is monitoring a square ⇄ butterfly interconversion. This would place the energy of activation at less than 15 kcal mol^{-1}. The recognition that both the square and the butterfly structures are arachno subunits of the well-known *closo*-$Mo_6(\mu_3\text{-}X)_8L_6$ unit, taken together with McCarley's[31] observation on the facile interconversions of rectangular and butterfly $Mo_4Cl_{12}^{3-}$ anions as a function of countercation, heightens our interest in the bonding, dynamics, and reactivity of these, the first Mo_4 alkoxide clusters.

Experimental Section

Physical Techniques. ^1H NMR spectra were recorded on a Nicolet NT-360 spectrometer at 360 MHz in dry and oxygen-free toluene-d_8, benzene-d_6, of methylene-d_2 chloride. ^{19}F NMR spectra were recorded on the same instrument at 340 MHz in the same solvents. ^{31}P NMR spectra were recorded on a Varian XL-100/Nicolet 1080 FT spectrometer at 40.5 MHz in the same solvents. All ^1H NMR chemical shifts are reported in ppm relative to the CHD_2 quintet of toluene-d_8 set at δ = 2.09, the ^1H impurity in benzene-d_6 set at δ = 7.15, or the CHD triplet of methylene-d_2 chloride set at δ = 5.33. All ^{19}F NMR chemical shifts are reported in ppm relative to the CF_3 singlet of CF_3COOH used as an external lock and set at δ = −78.9 ppm relative to $CFCl_3$. ^{31}P NMR chemical shifts are reported in ppm relative to external 85% H_3PO_4.

Infrared spectra were recorded on a Perkin-Elmer 283 spectrophotometer as Nujol mulls between CsI plates. Electronic absorption spectra were obtained with a Perkin-Elmer 330 spectrophotometer. Samples were run versus a solvent blank in matched 1.00-cm or 1.0-mm quartz cells.

Synthesis. All reactions were carried out under an atmosphere of dry and oxygen-free nitrogen by using standard Schlenk and glovebox techniques. Hexane and toluene were degassed and eluted from an activated copper catalyst and molecular sieve columns and then stored over sieves and under nitrogen. Phosphorus trifluoride was purchased from Pennwalt and used without purification. Acetyl fluoride was purchased from Aldrich, stored at −15 °C, and used without further purification. Trimethylphosphine was synthesized from triphenyl phosphite and a methyl Grignard reagent in dibutyl ether, distilled, and stored under vacuum. Chlorodimethylphosphine was purchased from Strem, degassed, and stored under vacuum prior to use. Diethyl ether, 1,2-dimethoxyethane, and THF were distilled from sodium benzophenone ketyl and stored under nitrogen and over sieves. Acetyl chloride and acetyl bromide were purchased from Aldrich, degassed, distilled, and stored over sieves and under nitrogen prior to use. Chloro-, bromo-, and iodotrimethylsilane were purchased from Aldrich, distilled, and stored under nitrogen prior to use. Iodotrimethylsilane is extremely sensitive to light, moisture, and air and was stored over copper metal and under nitrogen and kept in the dark at −15 °C to suppress radical reactions. Acetyl iodide was prepared from acetyl chloride and trimethylsilyl iodide by following standard literature procedures.[39] $Mo_2(O\text{-}i\text{-}Pr)_6$ was prepared by following literature procedures.[3] Elemental analyses were performed by Alfred Bernhardt Microanalytishes Laboratorium, Elbach, West Germany. A few comments about the elemental analyses of the chloride-containing compounds are in order. The analyses are low in C and high in Cl for $Mo_4Cl_3(O\text{-}i\text{-}Pr)_9$ and are in the reverse order for $Mo_4Cl_4(O\text{-}i\text{-}Pr)_9$. Both of these clusters are relatively insoluble in alkane solvents, which, of course, allows for their high-yield isolation. However, $Mo_4Cl_3(O\text{-}i\text{-}Pr)_9$ may, at times, contain small amounts of $Mo_4Cl_4(O\text{-}i\text{-}Pr)_8$ and vice versa.

$Mo_4F_2(O\text{-}i\text{-}Pr)_{10}$. This compound is thermally unstable at room temperature, and thus we have developed a special low-temperature reaction vessel for its high-yield isolation. The vessel consists of a 15-mm glass tube, sealed at one end, a coarse fritted disk in the center, and a constriction midway between the frit and the open end, which is tapered so as to fit Tygon tubing and a Kontes valve. This vessel is shown schematically in a figure elsewhere.[40]

$Mo_2(O\text{-}i\text{-}Pr)_6$ (0.500 g, 0.91 mmol) was completely dissolved in a minimum amount of toluene (ca. 5–10 mL). This solution was transferred to the reaction vessel and placed on top of the frit via micropipet. The vessel was then fitted with a removable Kontes valve with Tygon tubing and closed under nitrogen. The closed end of the vessel was then immersed in liquid nitrogen just below the frit. This provides the vacuum to pull the solution through the frit and into the closed end of the vessel, where it is frozen at −196 °C followed by evacuation of the reaction vessel. Acetyl fluoride (0.91 mmol, 1 equiv) was condensed into the vessel by using a calibrated vacuum manifold. The vessel was then sealed at the top by using a small hand torch and warmed to −20 °C. This temperature was maintained for 2 days to yield a nearly black solution. The vessel was then cooled to −78 °C and stored in a Dewar of dry ice, which was placed in the freezer. After 7 days the vessel was inverted and placed in liquid nitrogen just below the constriction to pull the filtrate into the receiving bulb. This procedure results in the deposition of a large mass of dark red-black crystals on the frit. The vessel was then sealed at the constriction with a hand torch, leaving the filtrate in the bulb and crystals on the frit (total yield 0.315 g, 68% based on Mo). Anal. Calcd for $Mo_4F_2O_{10}C_{30}H_{70}$: C, 35.54; H, 6.91; F, 3.75. Found: C, 35.47; H, 6.82; F, 3.69.

^1H NMR (toluene-d_8, −40 °C): $\delta(OCHMe_2)$ = 7.7, 5.6, 4.3 in a 2:1:2 ratio, isomer A; $\delta(OCHMe_2)$ = 7.5, 5.6, 4.5 in a 2:1:2 ratio, isomer B.

IR (cm^{-1}): 1340 w, 1320 w, 1210 w, 1125 m, 1110 s, 980 s, 945 s, 850 m, 832 m, 825 m, 650 m, 620 w, 601 m, 590 m, 460 m.

Alternate Synthesis. With use of the same type of reaction vessel and procedure, $Mo_2(O\text{-}i\text{-}Pr)_6$ (0.500 g, 0.91 mmol) was completely dissolved in toluene (5–10 mL). The solution was frozen at −196 °C, and PF_3 (0.91 mmol, 1 equiv) was condensed into the vessel by using a calibrated vacuum manifold. The reaction mixture was allowed to warm to −20 °C, and this temperature was maintained for 2 days. The vessel was then cooled to −78 °C and stored in a Dewar of dry ice. After 3 days 0.321 g of crystalline material was isolated by the previously described procedure.

$Mo_2F_2(O\text{-}i\text{-}Pr)_4(PMe_3)_2$. In a Schlenk reaction vessel $Mo_2(O\text{-}i\text{-}Pr)_6$ (0.520 g, 0.95 mmol) was dissolved in a minimum amount of toluene (10 mL). The solution was frozen at −196 °C, and PF_3 (1.90 mmol, 2 equiv) was condensed into the flask by using a calibrated vacuum manifold. Next, PMe_3 (1.90 mmol, 2 equiv) was condensed into the flask by using a calibrated vacuum manifold. The reaction mixture was warmed to −78 °C and stirred. This yields a bright purple solution due to the presence of $Mo_2(O\text{-}i\text{-}Pr)_6(PMe_3)_2$. After 1 h the reaction mixture was allowed to warm to room temperature, at which time the solution changed color to a brilliant red-orange. The reaction mixture was stirred for 2 h at room

(38) Ahmed, K. J.; Chisholm, M. H.; Rothwell, I. P.; Huffman, J. C. *J. Am. Chem. Soc.* **1982**, *104*, 6453.
(39) Schmidt, A. H.; Russ, M.; Grosse, D. *Synthesis* **1981**, 216.
(40) Chisholm, M. H.; Clark, D. L. *ACS Symp. Ser.* **1987**, *No. 357*, 3.1.

temperature, the volume was reduced by three-fourths, and the solution was cooled to −15 °C. Red-brown crystals were isolated after 6 days. A second crop of crystals was obtained by reducing the volume of the filtrate and cooling (total yield 0.32 g, 54% based on Mo). Anal. Calcd for $Mo_2F_2O_4P_2C_{18}H_{46}$: C, 34.92; H, 7.45; F, 6.14. Found: C, 34.62; H, 7.26; F, 6.29.

^1H NMR (toluene-d_8, 22 °C): $\delta(OCHMe_2)$ = 6.93, 4.55, equal-intensity septets; $\delta(OCHMe_2)$ = 1.69, 1.42, 1.40, 1.17, equal-intensity doublets ($^3J_{H-H}$ = 6.12 Hz); $\delta(PMe_3)$ = 1.44, doublet ($^2J_{P-H}$ = 8.9 Hz).

$^{31}P\{^1H\}$ NMR (toluene-d_8, 21 °C): $\delta(PMe_3)$ = −9.97, half of an expected AA′XX′ spectrum. Successful simulation gave $^2J_{P-F}$ = 115.7 Hz, $^3J_{P-F}$ = 34.9 Hz, $^3J_{F-F}$ = 3.0 Hz, and $^3J_{P-P}$ = 0.0 Hz. The signs of coupling constants were not determined.

^{19}F NMR (toluene-d_8, 22 °C): $\delta(F)$ = −99.2, half of an expected AA′XX′ spectrum.

$Mo_4Cl_3(O\text{-}i\text{-}Pr)_9$. In a Schlenk reaction vessel $Mo_2(O\text{-}i\text{-}Pr)_6$ (0.56 g, 1.03 mmol) was completely dissolved in a minimum amount of hexane (10 mL). At room temperature, 1.5 equiv (1.55 mmol) of acetyl chloride was added via a microliter syringe and the flask shaken vigorously. The color changed from yellow to burgundy, and heat was evolved. The flask was then allowed to stand undisturbed for several hours. On most occasions, small black crystals formed at room temperature. The flask was then cooled to −15 °C. After 2 days many large black crystals were collected by filtration and dried in vacuo (total yield 0.373 g, 72% based on Mo). Anal. Calcd for $Mo_4Cl_3O_9C_{27}H_{63}$: C, 31.73; H, 6.21; Cl, 10.41. Found: C, 31.30; H, 6.26; Cl, 11.68.

^1H NMR (toluene-d_8, 22 °C): $\delta(OCHMe_2)$ = 6.09, 5.91, 5.79, 4.52, 4.45, septets ($^3J_{HH}$ = 6.12 Hz) with relative intensities of 2:2:2:2:1, respectively; $\delta(OCHMe_2)$ = 1.97, 1.70, 1.58, 1.52, 1.44, 1.38, 1.15, 0.90, 0.89, equal-intensity doublets ($^3J_{HH}$ = 6.12 Hz).

IR (cm^{-1}): 1330 m, 1320 m, 1260 w, 1160 m, 1140 m, 1100 s, 969 s, 930 s, 845 s, 635 m, 610 w, 590 m, 569 w, 555 m, 530 w, 440 m, 360 w, 289 m, 232 m.

UV–visible absorption (hexane; λ_{max}, nm (ϵ, M^{-1} cm^{-1})): 990 (490), 680 sh (830), 526 (1700), 426 (2600), 260 (13 000), 200 sh (40 000).

Alternate Synthesis 1. In a Schlenk reaction vessel $Mo_2(O\text{-}i\text{-}Pr)_6$ (0.56 g, 1.03 mmol) was completely dissolved in hexane (30 mL). At room temperature, 1.5 equiv (1.55 mmol) of chlorotrimethylsilane was added via a microliter syringe with stirring. The flask was then immersed in a constant-temperature bath at 38 °C. After 12 h the solution had changed color from yellow to burgundy, indicating the formation of $Mo_4Cl_3(O\text{-}i\text{-}Pr)_9$. The volume of the solution was reduced by half and cooled to −15 °C. Black crystals were obtained after 3 days. A second crop of crystals was obtained by reducing the volume of the filtrate and cooled to −15 °C (total yield 0.320 g, 61% based on Mo).

Alternate Synthesis 2. This procedure was the same as that for the original preparation above except that Et_2O was the reaction solvent. Once the reaction started, the Et_2O began to boil and the flask was placed in an ice bath to stop the boiling and then warmed slowly to room temperature. After 3 h the stirring was ceased to yield a burgundy microcrystalline precipitate. The Et_2O was removed via cannula, and the solids were washed with more Et_2O and dried in vacuo. The yield was virtually quantitative from this preparation, and the products were of a high purity as judged by ^1H NMR spectroscopy.

$Mo_4Br_3(O\text{-}i\text{-}Pr)_9$. In a Schlenk reaction vessel $Mo_2(O\text{-}i\text{-}Pr)_6$ (0.97 g, 1.77 mmol) was completely dissolved in a minimum amount of hexane (25 mL). At room temperature, 1.5 equiv (2.66 mmol) of acetyl bromide was added via a microliter syringe and the vessel was shaken vigorously. The color changed from yellow to burgundy, and enough heat was evolved that the flask was very hot to touch. The flask was then allowed to stand and cool to room temperature undisturbed for several hours. After 2 h many large black crystals were present. The solution was then cooled to −15 °C. After 1 day large black crystals were collected by filtration and dried in vacuo (total yield 0.70 g, 68% based on Mo). Anal. Calcd for $Mo_4Br_3O_9C_{27}H_{63}$: C, 28.07; H, 5.45; Br, 20.75. Found: C, 27.96; H, 5.31; Br, 20.93.

^1H NMR (benzene-d_6, 22 °C): $\delta(OCHMe_2)$ = 6.25, 6.12, 5.93, 4.60, 4.46, septets ($^3J_{HH}$ = 6.12 Hz) with relative intensities of 2:2:2:2:1, respectively; $\delta(OCHMe_2)$ = 2.03, 1.69, 1.57, 1.45, 1.38, 1.09, 0.89, 0.88, doublets ($^3J_{HH}$ = 6.12 Hz) with relative intensity 1:2:1:1:1:1:1:1, respectively.

$^{13}C\{^1H\}$ NMR (toluene-d_8, 22 °C): $\delta(OCHMe_2)$ = 85.46, 84.87, 84.17, 83.69, 73.26, singlets of relative intensity 2:2:2:2:1, respectively; $\delta(OCH(CH_3)_2)$ = 27.78, 26.39, 25.75, 25.67, 25.04, 24.78, 24.64, 24.62, 24.49, equal-intensity singlets.

IR (cm^{-1}): 1330 m, 1320 m, 1160 m, 1139 m, 1100 s, 965 s, 930 s, 845 s, 630 m, 605 w, 590 m, 565 w, 550 m, 525 w, 440 m, 360 w, 275 m.

UV–visible absorption (hexane; λ_{max}, nm (ϵ, M^{-1} cm^{-1})): 980 (650), 680 sh (1000), 536 (2100), 432 (3300), 260 sh (13 000), 232 (48 000).

Alternate Synthesis 1. In a Schlenk reaction vessel $Mo_2(O\text{-}i\text{-}Pr)_6$ (0.56 g, 1.03 mmol) was completely dissolved in hexane solution (30 mL). At room temperature, 1.5 equiv (1.55 mmol) of bromotrimethylsilane was added via a microliter syringe with stirring. After 2 h the solution had changed color from yellow to burgundy, indicating the formation of $Mo_4Br_3(O\text{-}i\text{-}Pr)_9$. The volume of solution was reduced by half and cooled to −15 °C. Black crystals were obtained after 3 days. A second crop of crystals was obtained by reducing the volume of the filtrate and cooling to −15 °C (total yield 0.35 g, 58% based on Mo).

Alternate Synthesis 2. This procedure was the same as that for the original preparation above except that Et_2O was the reaction solvent. The reaction of $Mo_2(O\text{-}i\text{-}Pr)_6$ with acetyl bromide is very exothermic. The ether solution was cooled to 0 °C, and then acetyl bromide was added dropwise with stirring at 0 °C. After 1 h the solution was warmed to room temperature and stirred another 2 h. The stirring was ceased to yield a burgundy microcrystalline precipitate. The Et_2O was removed via cannula, and the solids were washed with more Et_2O and dried in vacuo. The yield was virtually quantitative from this preparation.

$Mo_4I_3(O\text{-}i\text{-}Pr)_9$. In a Schlenk reaction vessel $Mo_2(O\text{-}i\text{-}Pr)_6$ (0.360 g, 0.66 mmol) was completely dissolved in hexane (15 mL). This solution was cooled to −21 °C, and then 1.5 equiv (0.99 mmol in a 0.1 M hexane solution) of iodotrimethylsilane was added to the stirring solution via a pressure-equalized dropping funnel. The solution was stirred at −21 °C for 2 h, and the color changed from yellow to green-brown. The solution was then allowed to warm to room temperature and stirred another 4 h, to yield a brown microcrystalline precipitate. The flask was then cooled to −15 °C, and small brown crystals were isolated after 1 day (total yield 0.194 g, 45% based on Mo).

^1H NMR (toluene-d_8, 22 °C): $\delta(OCHMe_2)$ = 6.33, 6.24, 6.10, 4.52, 4.50, septets ($^3J_{HH}$ = 6.12 Hz) with relative intensities of 2:2:2:2:1, respectively; $\delta(OCHMe_2)$ = 2.02, 1.67, 1.71, 1.59, 1.42, 1.37, 1.07, 0.89, 0.86, equal-intensity doublets ($^3J_{HH}$ = 6.12 Hz).

IR (cm^{-1}): 1330 m, 1320 m, 1160 m, 1130 m, 1095 s, 960 s, 925 s, 845 s, 830 s, 630 m, 602 w, 560 w, 550 w, 519 w, 450 m.

UV–visible absorption (hexane; λ_{max}, nm (ϵ, M^{-1} cm^{-1})): 1000 (660), 560 (2800), 460 (4300), 410 (6600), 360 (8400), 260 (44 000).

$Mo_4Cl_4(O\text{-}i\text{-}Pr)_8$. In a Schlenk reaction vessel $Mo_2(O\text{-}i\text{-}Pr)_6$ (0.74 g, 1.35 mmol) was completely dissolved in toluene (15 mL). At room temperature, exactly 2 equiv (2.70 mmol) of acetyl chloride was added via a microliter syringe and the reaction vessel was shaken vigorously. The color changed from yellow to burgundy with evolution of heat, indicating the formation of $Mo_4Cl_3(O\text{-}i\text{-}Pr)_9$. After the mixture stood at room temperature for 2 h, the color appeared to darken. The solution was cooled to 0 °C for 24 h, which yielded many black crystals. The solution was then cooled further to −15 °C. This procedure of slow cooling is important to avoid precipitation of a powder. After 2 days, many large black crystals were isolated by filtration and dried in vacuo (total yield 0.464 g, 69% based on Mo). Anal. Calcd for $Mo_4Cl_4O_8C_{24}H_{56}$: C, 28.87; H, 5.65; Cl, 14.21. Found: C, 30.10; H, 5.69; Cl, 13.08.

^1H NMR (toluene-d_8, 22 °C): $\delta(OCHMe_2)$ = 6.25, 5.70, 4.80, extremely broad resonances with relative intensities of 2:1:1, respectively; $\delta(OCHMe_2)$ = 1.90, 1.60, 1.40, 0.75, extremely broad resonances of approximately equal intensity.

^1H NMR (toluene-d_8, −40 °C): $\delta(OCHMe_2)$ = 6.19, 5.71, 4.78, septets ($^3J_{HH}$ = 6.12 Hz) of intensity 2:1:1, respectively; $\delta(OCHMe_2)$ = 1.90, 1.53, 1.44, 0.68, equal-intensity doublets (^3J_H = 6.12 Hz).

IR (cm^{-1}): 1330 m, 1320 m, 1165 m, 1139 m, 1090 s, 975 s, 920 s, 840 s, 745 w, 735 w, 635 m, 625 m, 580 m, 500 m, 455 m, 365 w, 342 m, 302 s, 290 s, 232 s.

UV–visible absorption (CH_2Cl_2; λ_{max}, nm (ϵ, M^{-1} cm^{-1})): 1130 (590), 720 sh (900), 560 (1900), 425 (3300), 380 sh (2900), 260 sh (11 000).

Alternate Synthesis. In a Schlenk reaction vessel $Mo_4Cl_3(O\text{-}i\text{-}Pr)_9$ (0.50 g, 0.49 mmol) was dissolved in toluene (50 mL). At room temperature, 1 equiv of acetyl chloride (0.49 mmol) was added to the solution via a microliter syringe. The flask was shaken vigorously and then allowed to stand at room temperature for 3 h. The solution was then reduced in volume by half and cooled to −15 °C. After 2 days, black crystals were obtained (total yield 0.24 g, 51% based on Mo).

$Mo_4Br_4(O\text{-}i\text{-}Pr)_8$. In a Schlenk reaction vessel $Mo_2(O\text{-}i\text{-}Pr)_6$ (1.10 g, 2.01 mmol) was completely dissolved in toluene (15 mL). At room temperature, exactly 2 equiv (4.02 mmol) of acetyl bromide was added via a microliter syringe and the reaction vessel shaken vigorously. The color changed from yellow to burgundy with evolution of heat, indicating the formation of $Mo_4Br_3(O\text{-}i\text{-}Pr)_9$. After the mixture stood at room temperature for 2 h, the color darkened to green. One must be careful to be sure to allow the solution to turn green prior to cooling, otherwise $Mo_4Br_3(O\text{-}i\text{-}Pr)_9$ will crystallize as an impurity. The solution was cooled to 0 °C for 24 h, which yielded many black crystals. The solution was then cooled further to −15 °C. After 2 days, many large black crystals

were isolated by filtration and dried in vacuo (total yield 0.93 g, 78% based on Mo). Anal. Calcd for $Mo_4Br_4O_8C_{24}H_{56}$: C, 24.51; H, 4.79; Br, 27.18. Found: C, 25.43; H, 4.70; Br, 28.62.

^1H NMR: (toluene-d_8, 22 °C): $\delta(OCHMe_2)$ = 6.50, 5.95, 4.90, extremely broad resonances with relative intensities of 2:1:1, respectively; $\delta(OCHMe_2)$ = 2.00, 1.80, 1.60, 0.85, extremely broad resonances of approximately equal intensity.

^1H NMR (toluene-d_8, −20 °C): $\delta(OCHMe_2)$ = 6.35, 5.85, 4.80, septets ($^3J_{HH}$ = 6.12 Hz) of intensity 2:1:1, respectively; $\delta(OCHMe_2)$ = 1.89, 1.61, 1.49, 0.66, equal-intensity doublets ($^3J_{HH}$ = 6.12 Hz).

IR (cm^{-1}): 1330 m, 1320 m, 1115 m, 1130 m, 1090 s, 960 s, 940 s, 930 s, 920 s, 905 s, 845 s, 830 s, 625 m, 600 w, 580 m, 560 w, 540 w, 525 m, 460 w.

UV–visible absorption (CH_2Cl_2; λ_{max}, nm (ϵ, M^{-1} cm^{-1})): 1160 (500), 720 sh (1100), 580 (2200), 520 sh (2100), 435 (3700), 382 sh (4300), 260 sh (11 000), 240 (48 000).

Alternate Synthesis. In a Schlenk reaction vessel $Mo_4Br_3(O\text{-}i\text{-}Pr)_9$ (0.50 g, 0.43 mmol) was dissolved in toluene (50 mL). At room temperature, 1 equiv of acetyl bromide (0.43 mmol) was added to the solution via a microliter syringe. The flask was shaken vigorously and then allowed to stand at room temperature for 3 h, at which time the solution had turned from the burgundy (or perhaps port) color characteristics of the starting material to green, indicating the formation of $Mo_4Br_4(O\text{-}i\text{-}Pr)_8$. The solution was reduced in volume by half and then slowly cooled to −15 °C. After 2 days, black crystals were obtained (total yield 0.29 g, 58%).

$Mo_4I_4(O\text{-}i\text{-}Pr)_8$. In a Schlenk reaction vessel $Mo_2(O\text{-}i\text{-}Pr)_6$ (0.67 g, 1.23 mmol) was completely dissolved in toluene (15 mL), and the mixture was cooled to −78 °C. Exactly 2 equiv (2.46 mmol) of iodotrimethylsilane was added via a microliter syringe, and the reaction mixture was stirred and warmed to 0 °C. The color changed from yellow to green-brown, indicating the formation of $Mo_4I_3(O\text{-}i\text{-}Pr)_9$. After 2 h the solution was allowed to warm to room temperature and the color appeared to darken. The solution was reduced in volume by half and cooled to −15 °C for 24 h, which yielded black crystals. After 2 days, many large black crystals were isolated by filtration and dried in vacuo (total yield 0.32 g). There was always a trace amount of $Mo_4O_2I_2(O\text{-}i\text{-}Pr)_6$ present in the products on the basis of ^1H NMR spectroscopy.

^1H NMR (toluene-d_8, 22 °C): $\delta(OCHMe_2)$ = 6.25, 5.70, 4.80, extremely broad resonances with relative intensities of 2:1:1, respectively; $\delta(OCHMe_2)$ = 1.90, 1.60, 1.40, 0.75, extremely broad resonances of approximately equal intensity.

^1H NMR (toluene-d_8, −40 °C): $\delta(OCHMe_2)$ = 6.42, 5.96, 4.64, septets ($^3J_{HH}$ = 6.12 Hz) of intensity 2:1:1, respectively; $\delta(OCHMe_2)$ = 1.83, 1.77, 1.50, 0.60, equal-intensity doublets ($^3J_{HH}$ = 6.12 Hz).

IR (cm^{-1}): 1330 m, 1320 m, 1165 m, 1139 m, 1090 s, 975 s, 920 s, 840 s, 745 w, 735 w, 635 m, 625 m, 580 m, 570 m, 565 m, 500 m, 455 m, 365 w.

$Mo_4O_2I_2(O\text{-}i\text{-}Pr)_6$. In a Schlenk reaction vessel $Mo_2(O\text{-}i\text{-}Pr)_6$ (0.97 g, 1.75 mmol) was completely dissolved in toluene (50 mL), and the mixture was cooled to −78 °C. Exactly 2 equiv (3.50 mmol) of iodotrimethylsilane was added dropwise via a microliter syringe with stirring. The solution was allowed to warm slowly to room temperature with stirring. At room temperature the solution was dark green, indicating the formation of $Mo_3I_4(O\text{-}i\text{-}Pr)_8$. After 3 h at room temperature the mixture was warmed to 55 °C and stirred. After 2 days the color of the solution had turned to deep red-brown, indicating the formation of $Mo_4O_2I_2(O\text{-}i\text{-}Pr)_6$. The solution was reduced in volume by half and cooled to −15 °C. After 2 days a red-brown microcrystalline precipitate was isolated by filtration and dried in vacuo (total yield 0.45 g).

^1H NMR (toluene-d_8, 22 °C): $\delta(OCHMe_2)$ = 6.41 and 5.23, septets ($^3J_{HH}$ = 6.12 Hz) of relative intensity 2:1, respectively; $\delta(OCHMe_2)$ = 1.52, 1.37, 1.29, equal-intensity doublets ($^3J_{HH}$ = 6.12 Hz).

^1H NMR (benzene-d_8, 22 °C): $\delta(OCHMe_2)$ = 6.39 and 5.24, septets ($^3J_{HH}$ = 6.12 Hz) of relative intensity 2:1, respectively; $\delta(OCHMe_2)$ = 1.49, 1.32, 1.29, equal-intensity doublets ($^3J_{HH}$ = 6.12 Hz).

$^{13}C\{^1H\}$ NMR (toluene-d_8, 22 °C): $\delta(OCHMe_2)$ = 95.0, 89.0, singlets of relative intensity 2:1, respectively; $\delta(OCH(CH_3)_2)$ = 25.2, 25.1, 24.9, equal-intensity singlets.

IR (cm^{-1}): 1330 m, 1320 m, 1260 m, 1170 m, 1135 m, 1090 s, 1020 m, 910 s, 895 s, 840 s, 820 s, 600 m, 560 m, 470 m.

$Mo_4O_2Br_2(O\text{-}i\text{-}Pr)_6$. In a Schlenk reaction vessel $Mo_4Br_4(O\text{-}i\text{-}Pr)_8$ (0.500 g, 0.42 mmol) was dissolved in toluene (150 mL). The flask was fitted with a reflux condenser, and the solution was heated to 70 °C with stirring. After 3 days the color had turned from the green of $Mo_4Br_4(O\text{-}i\text{-}Pr)_8$ to red-brown, indicating the formation of $Mo_4O_2Br_2(O\text{-}i\text{-}Pr)_6$. The solvent was removed in vacuo, and the solids were washed twice with hexane to remove impurities. However, the solids almost invariably contained $Mo_4Br_4(O\text{-}i\text{-}Pr)_8$ impurities on the basis of ^1H NMR spectroscopy.

^1H NMR (toluene-d_8, 22 °C): $\delta(OCHMe_2)$ = 6.20, 5.15, septets ($^3J_{HH}$ = 6.12 Hz) of relative intensity 2:1, respectively; $\delta(OCHMe_2)$ = 1.46, 1.41, 1.25, equal-intensity doublets ($^3J_{HH}$ = 6.12 Hz).

$^{13}C\{^1H\}$ NMR (toluene-d_8, 22 °C): $\delta(OCHMe_2)$ = 91.5, 86.0, singlets of relative intensity 2:1, respectively; $\delta(OCH(CH_3)_2)$ = 25.0, 24.9, 24.4, equal-intensity singlets.

Crystallographic Studies. General operating procedures and listings of programs have been described previously.[41] A summary of crystal data is given in Table I.

$Mo_4F_2(O\text{-}i\text{-}Pr)_{10}$. A suitable crystal was cleaved from a larger crystal, transferred to the goniostat by using standard inert-atmosphere handling techniques employed by the Indiana University Molecular Structure Center, and cooled to −160 °C by using a gas-flow cooling system. A systematic search of a limited hemisphere of reciprocal space revealed a set of diffraction maxima with no apparent symmetry or extinctions, suggesting the triclinic space group $P\bar{1}$. Subsequent solution and refinement confirmed the choice.

The structure was solved by a combination of direct methods (MULTAN78) and Fourier techniques and refined by full-matrix least squares. Hydrogen atoms were not located but were included as fixed-atom contributors for all but the bridging OR group. An examination of the latter indicated that it either suffered from severe anisotropic motion or was disordered. Difference Fourier maps generated with the bridging OR removed failed to show discrete peaks but instead indicated that the group is highly fluxional in the solid state.

A final difference Fourier was featureless, the largest peak being 0.38 e/Å^3.

$Mo_4Br_3(O\text{-}i\text{-}Pr)_9$. A suitable small crystal was selected in the usual manner, transferred to the goniostat, cooled to −164.5 °C, and characterized. The crystal was monoclinic; the systematic extinctions identified the space group as $P2_1/c$.

The structure was solved by using direct methods, the four Mo atoms as well as the three Br atoms were located from the E map, and the remaining atoms were located in a difference Fourier phased on the heavy atoms. During the initial least-squares refinement it became evident that there was a disorder problem in the structure. Two peaks, Mo(4)* and Br(1)*, were located. Least-squares refinement varying the occupancies of these two peaks as well as of Mo(4), O(40), C(41), C(42), and C(43) indicated 15% occupancy for the first two atoms and 85% for the others. The occupancy was then fixed, and the least-squares refinement was completed. Hydrogen atoms were evident in a difference Fourier (except for the partial isopropoxy group). In view of the disorder problem the hydrogen atoms were included in idealized fixed positions.

A total of 4604 reflections having $F_o > 3\sigma(F_o)$ were used in the full-matrix least-squares refinement, which employed anisotropic thermal parameters on all non-hydrogen atoms. The final difference Fourier contained several peaks of about 1 e/Å^3, which was not surprising in view of the disorder.

$Mo_4Br_4(O\text{-}i\text{-}Pr)_8$. A suitable sample was transferred from a sealed tube to a goniostat by using inert-armosphere handling techniques. After transfer, the sample was cooled to −160 °C, at which temperature all measurements were made.

The structure was solved by a combination of direct methods (MULTAN78) and Fourier techniques and refined by full-matrix least squares. All hydrogen atoms were clearly discernable in a difference Fourier synthesis phased on the isotropically refined non-hydrogen coordinate. Hydrogen atoms were allowed to vary isotropically and all other atoms anisotropically in the final refinement.

The molecule possesses a crystallographic twofold axis, which passes through the central Mo–Mo bond of the backbone of the Mo_4 unit. A final difference Fourier synthesis was essentially featureless, with no peak exceeding 0.35 e/Å^3.

$Mo_4Cl_4(O\text{-}i\text{-}Pr)_8$. The crystals were black needles of various sizes, nearly all exhibiting marked fourfold symmetry. One or both ends of the needles were capped by a square pyramid, and one such end was cleaved from a needle of thickness 0.14 mm for the study. The sample was transferred to the goniostat and cooled to −126 °C by using standard inert-atmosphere techniques employed by the Indiana University Molecular Structure Center.

An E map phased on the results from MULTAN78 indicated a regular octahedron of molybdenum atoms with chlorines in each axial position. A Fourier synthesis phased on this model located the unique isopropoxy group in a face-bridging position of the octahedron. While these results were chemically surprising, least-squares refinement converged rapidly to $R(F)$ = 0.142 and $R_w(F)$ = 0.153, indicating an essentially correct structure. All intramolecular bond distances and angles were within "normal" ranges. An examination of intermolecular contacts, however,

(41) Chisholm, M. H.; Folting, K.; Huffman, J. C.; Kirkpatrick, C. C. *Inorg. Chem.* **1984**, *23*, 1021.

indicated a Cl···Cl contact of 1.7 Å, which was clearly not feasible.

Several precession photographs were taken of a second sample and examined carefully for doubling of one of the axes. Since there was no evidence for doubling, a large (0.45 × 0.55 × 0.70 mm) crystal was aligned on the goniostat and examined carefully for doubling of the axes, again with no success.

An examination of the final refinement indicated that the thermal parameters of Mo and Cl atoms not lying on the fourfold axis were larger by a factor of ca. 4 than those on the fourfold axis. This, and an examination of a Patterson synthesis, suggested the disorder, which was finally resolved. Mo(2) and Cl(4) were refined to 0.51 and 0.54 relative occupancies, with $R(F)$ dropping to 0.10. The occupancies were fixed at 0.50 for the remainder of the refinement.

Acknowledgment. We thank the National Science Foundation and the Wrubel Computing Center for support. D.L.C. was the 1983–1985 Indiana University SOHIO Graduate Fellow.

Registry No. I, 113794-50-6; II, 113794-55-1; III, 80878-94-0; IV, 80878-95-1; $Mo_2F_2(O\text{-}i\text{-}Pr)_4(PMe_3)_2$, 113794-51-7; $Mo_4Cl_3(O\text{-}i\text{-}Pr)_9$, 113794-52-8; $Mo_4I_3(O\text{-}i\text{-}Pr)_9$, 113794-54-0; $Mo_4I_4(O\text{-}i\text{-}Pr)_8$, 113794-53-9; $Mo_4O_2I_2(O\text{-}i\text{-}Pr)_6$, 113810-70-1; $Mo_4O_2Br_2(O\text{-}i\text{-}Pr)_6$, 113810-71-2; $Mo_2(O\text{-}i\text{-}Pr)_6$, 62521-20-4; PF_3, 7783-55-3; acetyl fluoride, 557-99-3; acetyl chloride, 75-36-5; chlorotrimethylsilane, 75-77-4; acetyl bromide, 506-96-7; bromotrimethylsilane, 2857-97-8; iodotrimethylsilane, 16029-98-4.

Supplementary Material Available: Listings of anisotropic thermal parameters, complete listings of bond distances and bond angles, and selected stereoviews for the molecules $Mo_4Br_4(O\text{-}i\text{-}Pr)_8$, $Mo_4Cl_4(O\text{-}i\text{-}Pr)_8$, $Mo_4Br_3(O\text{-}i\text{-}Pr)_9$, and $Mo_4F_2(O\text{-}i\text{-}Pr)_{10}$ (22 pages); listings of F_o and F_c values for the four compounds (63 pages). Ordering information is given on any current masthead page.

Contribution from the Departments of Chemistry, The Ohio State University, Columbus, Ohio 43210, and Indiana University, Bloomington, Indiana 47405

Electronic Structure and Bonding in Halide- and Alkoxide-Supported Tetranuclear Molybdenum Clusters

B. E. Bursten,*† M. H. Chisholm,*‡ and D. L. Clark‡

Received September 30, 1987

The bonding within square, rectangular, and butterfly tetranuclear molybdenum clusters, Mo_4^{12+}, supported in varying degrees by μ_3-X, μ_2-X, and terminal X ligands (X = Cl^-, OH^-) has been examined by nonempirical Fenske–Hall molecular orbital calculations. Mulliken populations of the canonical valence orbitals of the cluster framework are shown to vary with different ligand environments, which allows for the metal–metal bonding to be traced through successive stages of ligation. The calculations indicate that both capping and edge-bridging ligands cause the movement of charge out of the main metal–metal cluster-bonding orbitals, resulting in occupation of higher lying metal–metal nonbonding and antibonding orbitals. The bonding in the butterfly clusters $Mo_4(\mu_3\text{-}X)_2(\mu_2\text{-}X)_4X_6$ (X = OH^-, Cl^-) is shown to be dominated by the influence of the capping ligands whereas the square clusters of formula $Mo_4(\mu_2\text{-}X)_8X_4$ are shown to be dominated by edge-bridging ligands. Radial ligands on both the square and butterfly clusters are shown to be in competition for σ-density between metal–metal cluster bonding and radial metal–ligand bonding, and this phenomenon has been termed the *radial cluster influence*. It is shown that the rectangular cluster $Mo_4(\mu_2\text{-}Cl)_8Cl_4^{3-}$ is closely related to the square cluster of the same general formula, and the rectangular geometry can be understood as a result of a first-order Jahn–Teller distortion of the regular D_{4h} square structure in analogy with the case for the cyclobutadiene radical cation.

Introduction

Within the past several years a very rich and beautiful chemistry of halide- and alkoxide-supported tetranuclear molybdenum clusters has begun to emerge. One fascinating aspect of this chemistry is the similarity in structural geometries for halide- and alkoxide-supported clusters. Compounds of formula $Mo_4X_4(O\text{-}i\text{-}Pr)_8$ exhibit square and butterfly geometries in the solid state for X = Cl and Br, respectively, although the butterfly geometry is the dominant species in solution.[1,2] Similarly, the new chloromolybdate ions of formula $Mo_4Cl_{12}^{3-}$ display rectangular and butterfly geometries depending on the nature of the counterion, while the rectangular geometry seems to prevail in solution.[3] The iodomolybdate ion of formula $Mo_4I_{11}^{2-}$ also displays a butterfly geometry[4,5] closely related to that shared by $Mo_4Br_4(O\text{-}i\text{-}Pr)_8$ and $Mo_4Cl_{12}^{3-}$. The prototypical square and butterfly structures of general formula $Mo_4(\mu_2\text{-}X)_8X_4$ and $Mo_4(\mu_3\text{-}X)_2(\mu_2\text{-}X)_4X_6$ are shown in Figure 1. These general cluster types both contain Mo_4 units within a cube of X ligands and as such may be viewed as arachno derivatives of the well-known closo octahedral $Mo_6(\mu_3\text{-}X)_8X_6^{2-}$ cluster.[6-8] These cube–octahedral relationships are shown in I with the closo $Mo_6(\mu_3\text{-}X)_8^{4+}$ structure appearing in Ia. In the basic $Mo_6(\mu_3\text{-}X)_8^{4+}$ unit, the six molybdenum atoms define an octahedron, and the eight μ_3-X ligands symmetrically cap the triangular faces of the Mo_6 skeleton. The six metal atoms are also coordinated to six terminal ligands, which radiate from the vertices of the Mo_6 octahedron. By removal of two opposite

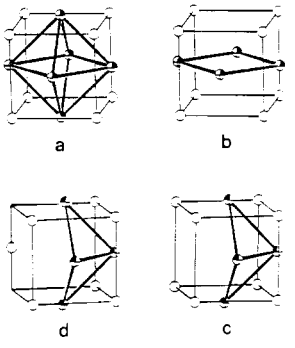

I

Mo vertices, one obtains the arachno Mo_4 square derivative shown in Ib, which yields eight doubly bridging X ligands while the terminal ligands radiate from the Mo vertices. In a similar fashion,

† The Ohio State University.
‡ Indiana University.

(1) Chisholm, M. H.; Errington, R. J.; Folting, K.; Huffman, J. C. *J. Am. Chem. Soc.* **1982**, *104*, 2025.
(2) Chisholm, M. H.; Clark, D. L.; Errington, R. J.; Folting, K.; Huffman, J. C. *Inorg. Chem.*, preceding article in this issue.
(3) Aufdembrink, B. A.; McCarley, R. E. *J. Am. Chem. Soc.* **1986**, *108*, 2474.
(4) Stensvad, S.; Helland, B. J.; Babich, M. W.; Jacobson, R. A.; McCarley, R. E. *J. Am. Chem. Soc.* **1978**, *100*, 6257.
(5) Glicksman, H. D.; Walton, R. A. *Inorg. Chem.* **1978**, *17*, 3197.
(6) Schafer, H.; von Schnering, H. G. *Angew. Chem.* **1971**, *385*, 75.
(7) Guggenberger, L. J.; Sleight, A. W. *Inorg. Chem.* **1969**, *8*, 2041.
(8) Healy, P. C.; Kepert, D. L.; Taylor, D.; White, A. W. *J. Chem. Soc., Dalton Trans.* **1973**, 646.

0020-1669/88/1327-2084$01.50/0